A&A 376, 621–640 (2001)
DOI: 10.1051/0004-6361:20010983

Astronomy & Astrophysics

Falling evaporating bodies in the β Pictoris system

Resonance refilling and long term duration of the phenomenon

P. Thébault[1] and H. Beust[2]

[1] Observatoire de Paris, Section de Meudon, 92195 Meudon Principal Cedex, France
[2] Laboratoire d'Astrophysique de l'Observatoire de Grenoble, Université J. Fourier, BP 53, 38041 Grenoble Cedex 9, France

Received 20 March 2001 / Accepted 15 June 2001

Abstract. The transient spectral absorption events that have been monitored for years towards the star β Pictoris have been interpreted as resulting from the transit across the line of sight of evaporating, star-grazing, kilometer-sized bodies (*Falling Evaporating Bodies*, or FEBs). These numerous star-grazers are thought to originate from the 4:1 and possibly 3:1 mean-motion resonances with a massive, Jovian-like planet orbiting the star at ∼10 AU on a moderately eccentric orbit ($e' \simeq 0.07$). A key issue concerning this scenario is its long-term duration over the age of the star, and therefore the refilling mechanism of the resonances. We first show here that, provided that the eccentricity of the planet orbit is slightly larger ($e' = 0.1$), the 3:1 resonance turns out to be the dominant source of FEBs rather than the 4:1. We show that letting the mass and the orbital semi-major axis of the planet vary leads to the conclusion that in order to correctly account for the observed FEB flux via the proposed mechanism, the planet needs to be Jovian-like and must not be located further away than ∼20 AU from the star. We then present long-term simulations of a collisional planetesimal disk showing that the collisions actually refill the resonances and are able to sustain the FEB activity over a very long time, as was previously suspected. Based on these simulations, constraints on the planet(s) and the disk population of planetesimals are derived.

Key words. stars: circumstellar matter – stars individual: β pic – methods: numerical – celestial mechanics – planetary systems: protoplanetary disks

1. Introduction

1.1. β Pictoris

The star β Pictoris (β Pic) is surrounded by a dusty and gaseous disk which has been intensively studied since its first detection 17 years ago (Smith & Terrile 1984). This system is still regarded as the best example of a possible extra-solar planetary system in its early dynamical evolutionary phase (see reviews by Artymowicz 1997; Vidal-Madjar et al. 1998; Lagrange et al. 2000). It is known today that the dusty particles viewed on the disk images are not a remnant of any primordial, more massive and opaque disk, but rather consist of second generation material continuously replenished from inside the disk by larger, planetesimal-like bodies, either by slow evaporation (Lecavelier et al. 1996) or by collisions (Artymowicz 1997).

Send offprint requests to: P. Thébault,
e-mail: Philippe.Thebault@obspm.fr

There has been in recent years some controversy regarding the age of β Pic. β Pic is a young main sequence A5 type star, and its age was initially estimated to be at least 10^8 yr. Paresce (1991), attributing the star's under-luminosity to a low metallicity effect, proposed an age of 2×10^8 yr. Conversely, Lanz et al. (1995) attributed the under-luminosity to extinction, proposing that β Pic was actually a pre-main-sequence star not older than 10^7 yr. Brunini & Benvenuto (1996) and Artymowicz (1997) concluded that any age between 10^7 and 10^8 yr could fit into the HR diagram constraints. Meanwhile, the stellar parameters of the star were remeasured by Crifo et al. (1997), who showed that the apparent under-luminosity of the star was formerly due to a bad estimate of the distance of the star. Vidal-Madjar et al. (1998), noting that βPic does not lie in the vicinity of any star-forming region, claimed that this was not compatible with an age of less than 3×10^7 yr, but Barrado y Navascués et al. (1999) carefully analyzed Hipparcos data from a moving stellar group tentatively associated with β Pic, concluding that the group was real,

and proposing an age of $20 \pm 10 \times 10^6$ yr, by estimation of the age of three M dwarfs associated with the group. In conclusion, it is still impossible to give a more accurate range than 2×10^7–10^8 yr.

1.2. Falling evaporating bodies

The study of the gaseous counterpart of the disk also provides strong indication for the presence of planetesimals orbiting β Pic. The survey of various spectral lines (Ca II, Mg II, Fe II, etc.) towards this star revealed that, apart from a deep central stable component, transient absorption features, usually redshifted, frequently appear or disappear. These additional features evolve within one day or even less (Boggess et al. 1991; Vidal-Madjar et al. 1994; Lagrange et al. 1996, and Refs. therein). These repeated spectral events have been successfully modeled as the signature of the evaporation of kilometer-sized bodies crossing the line of sight in the vicinity of the star, on star-grazing orbits. This scenario was extensively studied and modeled in the past years (Beust et al. 1990, 1996, 1998), and it is known today as the Falling Evaporating Bodies (hereafter FEB) scenario. Hence, independent arguments suggest that the presence of numerous planetesimal- or comet-like bodies within this disk is highly probable. This scenario is also suspected to apply to several Herbig Ae/Be stars (i.e., somewhat younger counterparts to main-sequence stars like β Pic) which exhibit spectral variations in metallic lines that look like those regularly monitored towards β Pic (Grady et al. 1997, 1999, 2000). However, the presence of strong stellar winds (typically $10^{-8}\ M_\odot\,\mathrm{yr}^{-1}$) makes potential FEBs much less easy to detect when they cross the line of sight, so that this question is still controversial (Beust et al. 2001).

The various types of spectral events have been classified in three different sets, which we will here briefly review (the reader might refer to Beust & Morbidelli 2000[hereafter BM00] or Beust et al. 1998 for a more complete description):

- Low velocity features (LVFs), which are deep (50% of the continuum) features with redshift velocities of the order of 10–50 $\mathrm{km\,s}^{-1}$, modeled as FEBs passing at less than $\sim$30 stellar radii (hereafter R_*), i.e. 0.24 AU from the star;
- High velocity features (HVFs), less deep (10% of the continuum), wider (several tens of $\mathrm{km\,s}^{-1}$), with infall velocities ranging from 100 to 300 $\mathrm{km\,s}^{-1}$. Their frequency is approximately 1/20 to 1/10 that of the LVFs events. These events are successfully modeled with the same scenario as for the LVFs, but assuming that the bodies pass very close to the star when being observed ($\lesssim 10\,R_*$);
- Very low velocity features (VLVFs), identified in the Ca II lines thanks to Ultra High Spectral resolution observations, with velocities ranging from -10 to $10\,\mathrm{km\,s}^{-1}$ (a negative value correspond to a blueshifted event), modeled as resulting from evaporating bodies crossing the line of sight at a distance to the star which may reach the evaporation limit for refractory material ($\sim$0.4 AU). The VLVFs are as deep as the LVFs but much narrower, and their frequency seems comparable.

1.3. The dynamical origin of FEBs

A key issue concerning the FEB scenario was the identification of a triggering dynamical mechanism capable of bringing numerous bodies on star-grazing orbits out of a Keplerian rotating disk on quasi-circular orbits. Various mechanisms were proposed, all of them involving the gravitational perturbations by at least one planet, preferably massive. They are discussed extensively in Beust & Morbidelli (1996[hereafter BM96]). The basic results concerning their application to the β Pic case are the following:

- The *Kozai resonance* is presently the main source of star-grazers in the Solar System (Bailey et al. 1992). It can nevertheless be ruled out as the main source for FEBs in the β Pic system for various reasons, essentially because the axisymmetry of this mechanism prevents it from reproducing the strong tendency towards redshifts in the observed FEB events;
- *Secular resonances* have been proposed a few years ago as a promising candidate, which might generate highly non-axisymmetric infalls (Levison et al. 1995). Demanding however the sole action of a secular resonance to be strong enough to generate numerous star-grazers requires the planetary system to adopt a very specific dynamical configuration that actually occurs by chance in the Solar System, but that has only low probability of occurring in another system. This scenario is therefore relatively non-generic. It can nevertheless not be straightforwardly ruled out, as the additional role of secular resonances in FEB dynamics could be important;
- *Mean-motion resonances* with a massive planet, which is the model we shall concentrate on hereafter, has been intensively studied in a few recent papers (BM96; BM00). This scenario is very generic and seems to be the most promising candidate today. Note that these models are not mutually exclusive. Morbidelli & Moons (1993), Moons & Morbidelli (1995) have indeed shown the very strong eccentricity pumping power of secular resonance *inside* mean motion resonance in the Solar asteroid belt. Such a picture could in fact apply to the β Pic case.

Following the work by Yoshikawa (1989), BM96 have analytically studied the topography of the 3:1 and 4:1 resonances with a moderately eccentric perturber. They have shown that these resonances are indeed the only ones able to bring the eccentricity of test particles almost up to 1. As shown by Yoshikawa (1989), the 5:2, 7:3 or 7:4 resonances may also cause significant eccentricity increases, but not sufficient for FEB generation. This issue was recently reinvestigated by Quillen & Holman (2000) who confirmed

that with a moderately eccentric perturber ($e \lesssim 0.15$), the 3:1 and 4:1 resonances are efficient sources of star-grazers, while for more eccentric perturbers, other resonances may become additional sources.

The application of this dynamic to β Pic was discussed in BM96 and extensively simulated in BM00. According to this model, the FEBs originate from the 4:1 resonance with a massive, Jovian-like planet orbiting the star on a moderately eccentric orbit ($e' \sim 0.05$–0.1). Under such conditions, the trapped particles are able to become star-grazers within $\sim 10^4$ revolutions of the planet. This scenario reproduces fairly well from a statistical point of view the dynamical characteristics of the FEBs that could be deduced from the observation of variable features.

In this model, the non-axisymmetry of the FEB infall is a direct consequence of the non-axisymmetry of the resonant librations when the perturbing planet's periastron is tilted with respect to the line of sight. The 4:1 resonance appears to be by far the most powerful resonance, since nearly every body trapped in it might reach $e \simeq 1$, whereas the effect of the 3:1 is significant only for particles having fairly large initial eccentricities ($\gtrsim$0.2–0.3, see below). These results have been confirmed by the numerical simulations of BM00, which, by following the evolution of a set of test particles, allowed us to constrain the orbital parameters of the perturbing planet, obtaining the best fit for $a' \simeq 10$ AU, $e' = 0.07$ and $\varpi' = -70°$. Here a' is the semi-major axis of the planet, e' its orbital eccentricity and ϖ' its longitude of periastron with respect to the line of sight. This dynamical configuration will be hereafter referred to as the nominal case. These simulation also allowed us to estimate the time-scale for generating FEBs from bodies initially orbiting on circular orbits, i.e. typically 10^5 yrs. In this fit, the most weakly constrained parameters are the planetary semi-major axis a'. $a' = 10$ AU is indeed a convenient value that allows the FEBs to originate not too close to the star ($\sim$4 AU), but choosing for example $a' = 15$ AU changes virtually nothing relating to the dynamical issue (see discussion Sect. 3). Similarly, in BM00, the mass ratio between the planet and the star was fixed at 0.001. As the mass of the star is approximately 1.7 $M_\odot$, this makes a planet with 1.8 Jupiter masses. This parameter is also weakly constrained and should be considered as accurate within one order of magnitude only (see Sect. 3). In the following simulations, we will first assume $a' = 10$ AU and $\mu = 0.001$.

A first estimate of the statistical properties of this model, in terms of both distribution of FEBs velocities and number of expected events, under the conditions of the nominal case, has been performed by BM00. These estimations of the FEB generating mechanism's efficiency allowed the authors to estimate the real number density of objects in the physical planetesimal disk required to reproduce the observed flux of evaporating bodies. For the nominal case, the obtained values range from 2×10^7 to 2×10^8 bodies per AU in the 4:1 resonance.

BM00 were also able to estimate the minimum size $R_{\rm FEB}$ of the evaporating FEBs, typically 10–20 km, though this value is poorly constrained, as it strongly depends on the still conjectural composition and structure of the FEB bodies.

1.4. The mass and time-scale problem

An important problem to overcome is the duration of the FEB episode. Indeed, 10^5 yr is the characteristic time for a given body to become FEB. If it did not evaporate due to close periastron passages, it would return to $e \simeq 0$ within another 10^5 yr and furthermore re-initiate another eccentricity increase cycle. This picture does not hold, basically because the repeated close periastron passages during the first eccentricity-increase episode cause the total evaporation of the body before it can return to small eccentricities. The net result of this process on the population of the resonance is to clear out the resonance of FEB candidates within a similar time-scale, i.e. 10^5 to 2×10^5 yr. The simulation result displayed in Fig. 2 from BM00 indeed shows a peak of activity at $\sim 1.5 \times 10^5$ yr and a strong decrease afterwards.

The problem is that this time-scale is only a small fraction of the estimated age the system. As noted in BM96, this clearing out time-scale could actually be a few times larger because the eccentricity of the perturbing planet may be subject to secular fluctuations, and therefore the efficiency of the FEB generating mechanism could drastically drop at some epochs. The net result is nevertheless unchanged, i.e., within the age of the system, the resonance should have cleared out and the FEB activity should have ceased a long time ago, or being very low today. Matching the observed number of events with a very low post-peak FEB activity would require far too high a planetesimal density in the disk. We are thus left here with an order of magnitude quantitative problem; a problem that might be solved by either finding a powerful mechanism for refilling the resonance, or a mechanism which might increase the efficiency of the FEB generating process, and thus reducing the required number density of bodies by several orders of magnitude, or by finding a mechanism able to extend the duration of the high activity episode by at least a factor 10.

In a first attempt, BM00 made a simple analytical study of the refilling process. From the values of $R_{\rm FEB}$ and the linear density $N_{\rm in}$ of bodies inside the resonance, depending on the refilling mechanism assumed, it is possible to derive the outside density $N_{\rm out}$ necessary for a steady-state refilling. Then, assuming a size distribution of the planetesimals, it is possible to estimate (though with large uncertainty) the linear mass density of planetesimals $M_{\rm plan}$ in the disk.

Basically, two mechanisms may refill the resonances: migration of the perturbing Jovian planet and mutual collisions among planetesimals. Of course both are not mutually exclusive. The migration model depends critically

on the migration velocity assumed. With the very slow velocities compatible with migrations caused by planetesimal scattering (typically 10^{7}–10^{-8} AU yr^{-1}; see Liou & Malhotra 1997; Murray et al. 1998), the necessary planetesimal density within the disk for an efficient refilling is far too high for being realistic. Conversely, migration models involving a strong tidal interaction with a dense gaseous disk (Ward 1997; Trilling et al. 1998), with much higher migration velocities ($\sim 10^{-5}$ AU yr^{-1}) require much less mass, but the gas mass needed for such an interaction exceeds by far the observed gas density in the β Pictoris system. Recently, Quillen & Holman (2000) investigated numerically the refilling by planetary migration, assuming arbitrarily an intermediate migration velocity ($\sim 10^{-6}$ AU yr^{-1}). With such a migration speed, less mass is needed in the disk, but the planet is expected to end up in the star within $\sim 10^{7}$ yr at most. As the star is at least twice as old, it is hard to believe this to be presently active in the β Pic system. If planetary migration is currently active in the β Pic system, then its speed is necessarily too low to account for resonance refilling on its own.

On the other hand, collisions seem to be able to refill the resonances, but BM00 estimated that an effective refilling of the 4:1 resonance would require large, and maybe irrealistic, planetesimal densities of the order of a few 10^{8} bodies per AU. Converted to linear mass density, assuming $R_{\rm FEB} = 15$ km, this becomes $7 \lesssim M_{\rm plan} \lesssim 70\ M_{\oplus}\,{\rm AU}^{-1}$. These values seem rather reasonable when compared to those of the Solar System, though they seem in disagreement with the gap of dust particles which seems to be observed in the inner βPic disk (see e.g. Artymowicz 1997; Pantin et al. 1997). However, it is not straightforward that such a dust depletion might be directly linked to kilometer-sized bodies depletion, as it seems rather hazardous to directly extrapolate this dust depletion over 10 order of magnitudes up to the kilometer-sized planetesimals. This particular problem will be the subject of forthcoming work and, in a first approach, we will here consider the 7 to 70 $M_{\oplus}\,{\rm AU}^{-1}$ mass range as an only marginally realistic plausible value.

Other mechanisms that make planetesimals drift in the semi-major axis may be invoked, but they appear to be far too weak to play a significant role. For example, the Yarkovsky effect, i.e., a non-zero radiation pressure balance due to temperature differences between regions on the surface of the body (see Vokrouhlický & Farinella 1999, and Refs. therein) causes a secular semi-major axis decay that may let new bodies enter the resonance. In their nonlinear theory, Vokrouhlický & Farinella (1999) estimate the decay rate to $\sim$0.02 times a normalization value. Scaling their work to a 10 km-sized body feeling the radiation flux of β Pic at 5 AU, we find this value to be $\sim 10^{-7}$ AU yr^{-1}, which sets the semi-major axis decay rate to a few $\sim 10^{-9}$ AU yr^{-1}, i.e. even less than the smallest value obtained from planetary migration. As a matter of fact, we will see in the following that the typical collision time in the planetesimal disk is $\sim 5 \times 10^{5}$ yr, i.e. a $\sim 10^{-1}$ AU jump every $\sim 5 \times 10^{5}$ yr. Collisions largely overcome the Yarkovsky effect. Actually this effect plays a significant role only in collisionless environments, and on time-scales comparable to the age of the Solar System. Clearly this situation does not apply here.

The present paper presents some possible clues to these unsolved issues. We will first reconsider the basic FEB generating mechanism, but focusing now on the 3:1 resonance in addition to the 4:1 one (Sect. 2). The contribution of the 3:1 had been too quickly overlooked in previous studies (BM96; BM00). We show here that its global effect might, under certain circumstances, outstrip that of the 4:1 resonance, thus lowering the number of planetesimals required and extending the duration of the FEB activity period. In Sect. 3, we discuss how these results change if we let the mass and the semi-major axis of the perturbing planet vary, and we put some constraints on these parameters. We will also reconsider the mutual collision refilling effect, which cannot be fully estimated by simple order of magnitude analytical computations, by performing accurate numerical simulations (Sect. 4) which show a tendency to further increase the FEB episode duration. These results will then be discussed and reinterpreted in Sect. 5 and some perspectives will be given in Sect. 6.

2. The 3:1 resonance as an alternative source of FEBs

2.1. Long-term simulations for the nominal case

The FEB flux estimates of BM00 were obtained, for the 3:1 and 4:1 resonances, by considering 10 000 bodies trapped inside each resonance. Thus, what these simulations actually estimated was the efficiency of each resonance and it lead to neglecting the role of the 3:1 resonance because its efficiency (for star-grazer generation) on a fixed population of bodies is only 0.5%, which is negligible compared to that of the 4:1 ($\sim$40%). But comparing the efficiency of the resonances is not equivalent to comparing their actual global effect, since there is another parameter that has to be taken into account, i.e., the width of the resonance. For the nominal case (i.e., for bodies with $e \leq 0.1$), the radial extension of the 3:1 resonance (2.5×10^{-2} AU) is many times larger than that of the 4:1 (see BM96). The greater extension of the 3:1 resonance may partly compensate its weaker efficiency, as for the same linear density of bodies, more bodies are expected to be trapped into the 3:1 resonance than in the 4:1.

Thus, in order to quantitatively compare the global effect of each resonance, new simulations have been performed considering systems with the same fixed radial particle density Λ. In both cases, the initial eccentricities were sorted between 0 and 0.1, and the inclinations between 0 and 3°. The conditions are those of the nominal case. We arbitrary fixed $\Lambda = 2 \times 10^{6}$ bodies AU^{-1} in order to have enough particles in each resonance: for the 4:1 resonance, 11 428 bodies were initially taken with semi-major axes randomly sorted between 3.96486 and 3.97058 AU; these

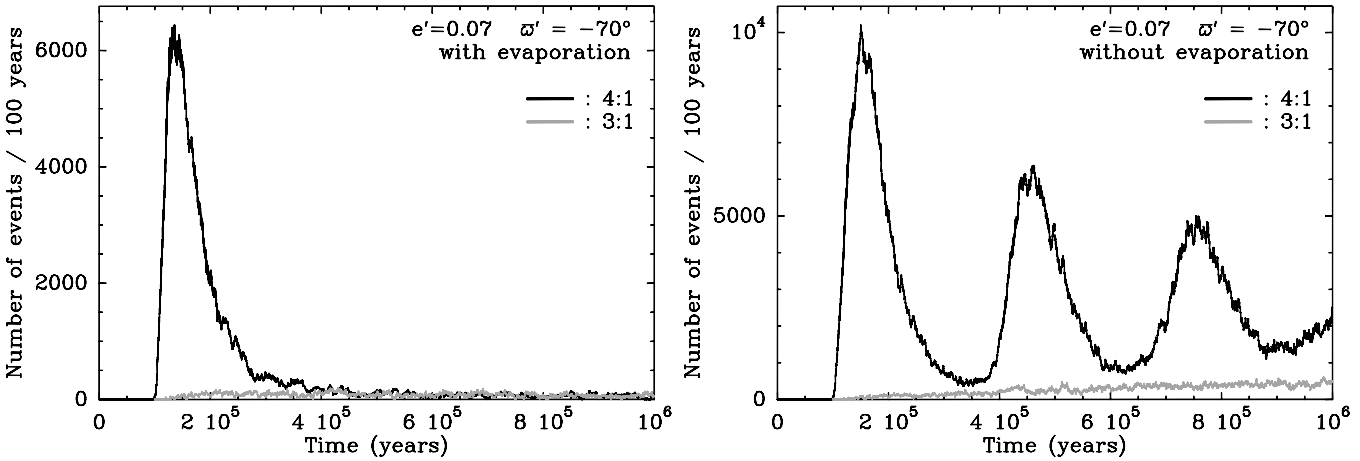

Fig. 1. Global histograms of FEB flux over 10^6 yr for the 4:1 (black lines) and the 3:1 (grey line) simulations, for a perturber with eccentricity $e' = 0.07$. The left plot represents the physical situation where the evaporation of bodies when entering the FEB regime is taken into account, so that individual bodies no longer generate FEB spectral events when fully evaporated. For comparison, the right plot shows the fluxes that would be expected if the bodies were never destroyed.

limits correspond to the exact borders of the 4:1 resonance zone at $e = 0.1$ for the nominal case. In BM00, the particles were initially taken over a more restricted semi-major axis range (10^{-3} AU wide) in order to ensure that most of the simulated particle were actually trapped in the resonance. As a matter of fact, the characteristic V shape (see BM96) of the resonance in (a, e) space causes roughly half of the 11 428 particles (basically, those at lowest eccentricity) we choose here to be in fact not trapped in the resonance and to have virtually no chance of becoming FEBs. However, this is the price to pay if we want to deduce reliable statistics from our simulations. Taking particles over a narrower range inside the resonance just ensures that a larger fraction of the particles are actually trapped, but tends to underestimate the total number of FEBs expected from the resonance.

For the 3:1, 56 557 bodies were taken with $4.79128 \leq a \leq 4.82899$ AU. As in BM00, the numerical integration was performed using the Mixed Variable Symplectic integrator (*swift_mvs*) developed first by Wisdom & Holman (1991) and furthermore by Levison & Duncan (1994). Contrary to BM00, the integration was carried on up to 10^6 yr, in order to see the long-term behavior. Note that we assume here that the orbit of the perturbing planet is fixed, which might not be relevant on such a time-scale if other (giant) planets are present in the system.

When computing the FEB events generated by individual bodies, we take into account their gradual evaporation using the approximate rules described in BM00, i.e. basically considering that the body evaporates when it enters the dust sublimation zone $d \lesssim 0.4$ AU, and that the evaporation rate at 0.15 AU is 3×10^7 kg s^{-1}, the latter value being dictated by simulations able to reproduce the observed events (Beust et al. 1998).

Figure 1 presents the compared FEB flux of the two resonances. It shows clearly that in the 4:1 integration, a first FEB events peak appears after $\sim 1.5 \times 10^5$ yr. This is basically the time needed for bodies to see their eccentricity brought up to $\sim$1, starting from $\sim$0. If the bodies would never be destroyed by evaporation, this peak would appear to be repeated every $\sim 3 \times 10^5$ yr (Fig. 1), which obviously corresponds to the period for the whole eccentricity increase and decrease cycle for resonant bodies. Now, if we take into account the evaporation as described above, only the first peak is observed, as very few bodies are able to survive after a full high-eccentricity episode.

In sharp contrast to the 4:1 case, the flux of events due to the 3:1 resonance does not present a strong peak. Conversely, the average number of events remains almost constant, and even slightly increases for more than 5×10^5 yr. Consequently, the 3:1 induced events are as numerous as the 4:1 ones after 4×10^5 yr. The total number of events due to the 4:1 resonance over 10^6 yr integration remains much larger than those due to the 3:1, so that the results of BM00 do not appear quantitatively affected: the 3:1 resonance is only a minor, additional source of FEBs.

In both cases, we also estimated the efficiency f of the FEB generation mechanism as the proportion of initial particles that reached the FEB state (i.e., a periastron value inside the dust evaporation limit, 0.4 AU) before the end of the run. We get $f = 0.2$ in the 4:1 case and $f = 0.011$ in the 3:1 case. This shows clearly that the 4:1 resonance is a much more powerful mechanism.

The efficiency $f = 0.2$ for the 4:1 case differs from the $f = 0.4$ value derived in BM00. However, that value was derived on the *resonant* particles only, for a population taken over a more restricted semi-major axis range in order to ensure that more particles are actually trapped. We preferred here to compute the efficiency on the *total* number of particles simulated, as this way appears more appropriate for further disk population estimates. Indeed, due to the shape of the resonance in (a, e) space, only $\sim$50% of the particles simulated here fall in the 4:1 resonance, so that if we restrict ourselves to those particles, we are back to an efficiency of 40% as before.

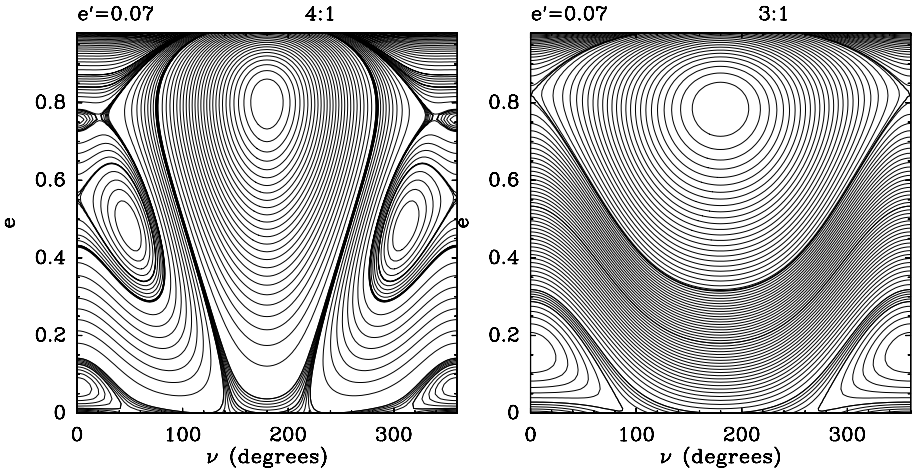

Fig. 2. Theoretical level curves of the resonant Hamiltonian, for trapped particles with negligible libration level in a ($\nu = \varpi - \varpi'$, e) diagram, for a perturber eccentricity $e' = 0.07$, and for the 4:1 (left) and 3:1 (right) mean-motion resonances. As the Hamiltonian is a constant of motion, the motion of each resonant particle follows one of these level curves.

2.2. Theoretical aspects

The numerical integrations reveal striking long-term behavior differences between the 4:1 and the 3:1 mean-motion resonances, which may be explained theoretically. The secular motion of a particle trapped in a mean-motion resonance is characterized by the libration of a critical angle usually named σ around an equilibrium position; non-resonant orbits are characterized by the circulation of σ (see BM96, for details). The libration of σ around an equilibrium position induces secular oscillations of the semi-major axis a.

If the perturber's orbit is circular ($e' = 0$), then a secular invariant N appears which prevents the eccentricity from undergoing drastic changes. The only secular motion of the particle is the resonant libration. If $e' \neq 0$, then N is no longer conserved, but to first order, the motion is qualitatively the same, i.e., libration of a, e and σ around equilibrium values. On a longer time-scale, the eccentricity of the perturber causes nevertheless this libration equilibrium to divert from its initial value, reaching sometimes high eccentricity values, depending on the resonance under consideration and on the value of e'. However, during this long-term evolution, another adiabatic invariant (named J) is conserved which represents roughly the amplitude of the libration motion (Morbidelli & Moons 1993; Moons & Morbidelli 1995).

Figure 2 illustrates this dynamic in the limiting case of negligible libration amplitude. In that case, the value of σ and a are fixed, and if we restrict ourselves to a planar problem, the secular Hamiltonian appears to be monodimensional, depending only on the value of the eccentricity e and of the longitude of the periastron ϖ. The dynamics may then be illustrated in a planar (ν, e) diagram, where $\nu = \varpi - \varpi'$. The resonant particles follow level curves of the Hamiltonian, exploring them clockwise. In Fig. 2 we have drawn these level curves of the Hamiltonian, for the 3:1 and 4:1 resonance respectively, and for $e' = 0.07$. In each point, the Hamiltonian was numerically evaluated as explained in Moons (1994).

From Fig. 2 it appears obvious when following the level curves that nearly every particle trapped in the 4:1 resonance in such conditions will evolve up to $e \simeq 1$ (i.e., FEB state). Conversely, for the 3:1, only those particles initially at $e \gtrsim 0.3$ may evolve to such a state. This basically explains why the 4:1 is much more powerful than the 3:1.

If the libration level of the particle is not zero, the motion of the particle in the (ν, e) diagram does not follow the same level curves as in Fig. 2, but other curves corresponding to another adiabatic invariant J. Building a similar plot for non-zero libration amplitudes is possible but less easy. Qualitatively speaking, if the libration amplitude is moderate, the motion remains roughly unchanged, the particle just slightly wanders around the curves of Fig. 2 and undergoes a FEB-like evolution. This wandering has an important consequence for the 3:1 resonance: particles initially somewhat below the $e_{\min} \simeq 0.3$ threshold may still evolve toward high eccentricities, thanks to their wandering around the theoretical zero amplitude curves. This explains why the simulation yields a limited number of FEB events, although the initial eccentricities of the particles were chosen $\leq$0.1!

Conversely, particles with large libration amplitudes indeed do not undergo a FEB-like evolution, and remain at low eccentricity. This fact limits the efficiency of the eccentricity pumping motion in the 4:1 resonance. This is why the efficiency of the 4:1 resonance remains significantly below 100%, contrary to what Fig. 2 suggests.

The low efficiency of the 3:1 resonance also explains why its activity does not drop after a first peak, like the 4:1. The FEB activity is too low to significantly clear the resonance over 10^6 yr. Moreover, as the process that makes new bodies enter the dynamical evolution toward large eccentricities is basically random (wandering due to libration), the corresponding frequency of FEB activity is not expected to present a pronounced secular cycle over a few 10^5 yr as in the 4:1.

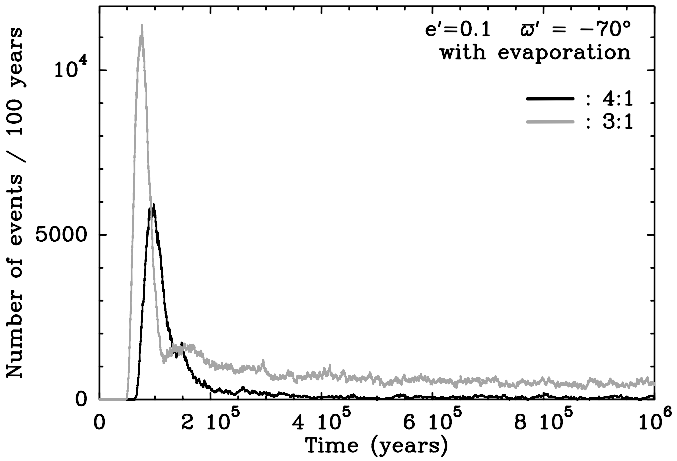

Fig. 3. Same as Fig. 1 with evaporation (left), but for $e' = 0.1$.

2.3. Improved performances for a more eccentric perturber

The key parameter controlling the potential FEB activity of the 3:1 resonance over an initially moderately eccentric population is the minimum eccentricity value $e_{\min}$ reached in a phase diagram like Fig. 2 by those Hamiltonian level curves which conduct up to $e \simeq 1$. This value is reached for $\nu = 180°$, and it is very sensitive to the perturber's eccentricity e'. This may be seen on plots similar to Fig. 2 for $e' = 0.05$ and $e' = 0.1$, presented in BM96.

The efficiency of the 3:1 resonance is almost zero for $e' \lesssim 0.05$ (for $e' = 0.05$, we have $e_{\min} \gtrsim 0.4$), but it increases extremely rapidly as e' just slightly increases. For $e' = 0.1$ (a case which could appear dynamically close to $e' = 0.07$), we have $e_{\min} \simeq 0.22$ only. This potentially shows that for the same initial population, more bodies may be to subject a FEB-like dynamical evolution than for $e' = 0.07$.

New simulations, identical to those described above, but with $e' = 0.1$ have thus been performed (Fig. 3), which clearly confirm this strong dependency of the 3:1 resonance's efficiency to e'. The value of the maximum FEB flux appears increased by a factor 30 compared to the $e' = 0.07$ case. Conversely, it can be noted that the 4:1 resonance's efficiency remains remarkably identical in the two cases. This basically comes from the fact that for the 4:1 resonance $e_{\min}$ is virtually 0 in both cases. Hence changing e' from 0.07 to 0.1 does not yield a significant gain in FEB efficiency for the 4:1 resonance.

Consequently, the 3:1 resonance now turns out to be the dominant source of events. The maximum total flux of FEB events due to the 3:1 is approximately 2 times higher than the 4:1 one. Note however that the 4:1 resonance still remains more efficient than the 3:1, the latter having a lower efficiency on a given population. Indeed, if both resonances were equally efficient, the ratio between their peak activity levels would correspond to the ratio of the populations we chose, i.e. ∼5. Here the 3:1 is only twice as active as the 4:1, showing that it is less efficient. It nevertheless dominates the flux because it is more crowded thanks to its larger extension in the semi-major axis.

The long-term behavior of the 3:1 generated events is less favorable than for the nominal case. There is now a sharp drop (∼80%), after $\sim 10^5$ yr. But after this drop, the FEB level then becomes more stable, though still progressively decreasing by another factor 2 in 10^6 yr. Nevertheless, this "lower level" regime is on average still equal to 15% of the *maximum* flux of the 4:1 in the nominal case. This means that the 3:1 resonance might thus sustain a significant FEB activity for 10^6 yr or even more. This is a significant gain in duration, of approximately one order of magnitude, compared to the nominal 4:1 case. The corresponding density of bodies required in the "real" disk might be estimated to be 1/0.15 the density estimated for the peak 4:1 activity, which gives us a 10^8 to 10^9 per AU range. Nevertheless, this 3:1 activity vanishes after a few 10^6 years, which is still too short compared to the age of the system.

Taking e' significantly above 0.1 would obviously even improve the efficiency, but this is clearly not a generic assumption, as such eccentricity values lie well above those of the giant planets of the Solar System. Conversely, $e' = 0.1$ is still a realistic value, as the secular orbital evolution of Jupiter and Saturn, mainly due to their mutual perturbations, cause them to reach such eccentricity values. Note however that assuming a similar situation towards β Pic implies the presence of at least two giant planets of comparable masses.

2.4. The velocity distribution of the events

The conditions of the nominal case ($a' \simeq 10$ AU, $e' = 0.07$, $\varpi' = -70°$) were fixed in BM00 in order i) to get numerous enough FEBs from a realistic configuration, and ii) to get a convenient fit of the observed velocity distribution of the spectral FEB events. The key parameter controlling this last point is ϖ', the longitude of periastron of the planet with respect to the line of sight. Fixing $\varpi' = -70°$ yields a fairly good fit of the observational conditions for all kinds of observed events (HVFs, LVFs and VLVFs), and for events generated from the 4:1 resonance. This may be seen from Fig. 8 from BM00. As we know that with $e' = 0.1$, the 3:1 is able to generate numerous events, it is now worth wondering whether this fitting condition also apply to the events generated from that resonance.

This is illustrated in Fig. 4, which shows the redshift velocities of all events computed from the simulation as a function of the distance they occur, i.e., the stellar distance of the FEBs when crossing the line of sight. This figure must be compared to Fig. 8 from BM00 which is the same for the 4:1 and $e' = 0.07$ (with $e' = 0.1$ the resulting plot for the 4:1 is almost identical). We note that the observational boxes are still globally fitted, but less perfectly that for the 4:1. The main "belt" of events is thicker, and moreover, it extends now well

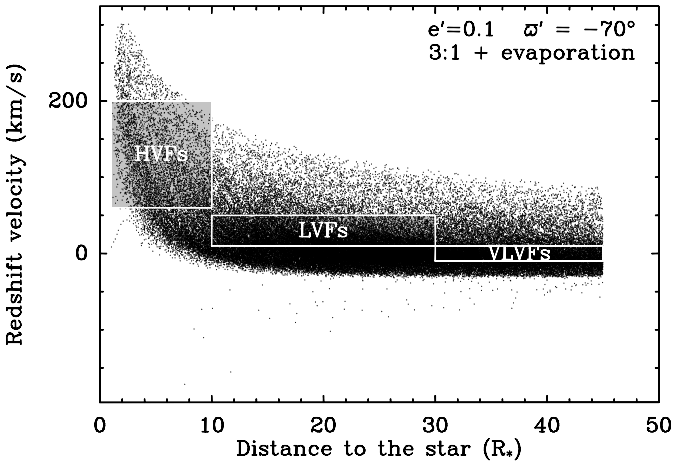

Fig. 4. Plot of the redshift velocity off all FEB events generated from the 3:1 resonance, as a function of their stellar distance, for the dynamical conditions written on the plot, and where the gradual evaporation of bodies was taken into account, as for Fig. 3. The conventions for the plot are the same as similar figures from BM00: the gray boxes represent the approximate combined observational/model-dependent constraints of the different kinds of observed spectral events (HVFs, LVFs, VLVFs).

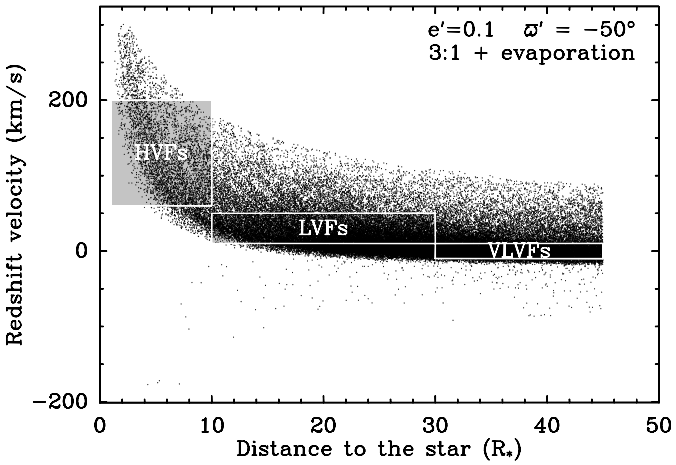

Fig. 5. Same as Fig. 4, but with now $\varpi' = -50°$. The fit is better, for a global number of events roughly identical.

below the boxes, toward blueshifted velocities. The fit may be improved changing ϖ'. This is illustrated in Fig. 5, which is equivalent to Fig. 4 but with $\varpi' = -50°$. The fit of the boxes is now better and may be considered as acceptable. Note however that according to this result, we should expect to observe a significant number of LVF-type (i.e., deep and strong) events at redshift velocities around 100 $\mathrm{km\,s^{-1}}$, which was never the case.

Conversely, we note in Fig. 5 a limited number of blueshifted events, well isolated from the main belt. As noted in BM00, blueshifted LVF-like components have been sometimes observed toward βPic (see Crawford et al. 1998). These events could not been explained with the sole action of the 4:1 resonance, but it was shown in BM00 that adding a terrestrial-like planet orbiting the star well inside the orbit of the main Jovian-like planet could help generate these events. Here we see in Fig. 5 that these events are naturally generated by the 3:1 resonance, together with a redshifted main belt, without invoking additional planets. As a matter of fact, Fig. 5 can be compared to Fig. 12 from BM00.

A careful analysis of the origin of these additional blueshifted events reveal that they are all due to bodies that first generate events in the main belt and then generate blueshifted ones. These are bodies that have passed through their minimum periastron distance following the curves of Fig. 2, and have $\nu = \varpi - \varpi'$ values above 180°, with (increasing) periastron values still well inside the dust evaporation zone. Blueshifted events occur when the FEBs cross the line of sight *after* periastron, i.e., for $\varpi < 0$. This corresponds to $0 < \nu < -\varpi'$ and $180° - \varpi' < \nu < 360°$. With $\varpi' = -70°$, this gives $0 < \nu < 70°$ and $250° < \nu < 360°$. The second range is the right one. If $\varpi' = -50°$, then we get blueshifted events as soon as $\nu > 230°$. We should then have more blueshifted events with $\varpi' = -50°$, which indeed appears to be the case in the runs.

This behavior was not seen with the 4:1 simulations for basically two reasons: first, with the 4:1 resonance the minimum periastron reached by the bodies is on average smaller than for the 3:1. This can be seen in Fig. 5: HVFs are much less numerous than LVFs and VLVFs. When the bodies reach smaller periastron values, they better evaporate; second, the duration of the high-eccentricity phase in the 3:1 cycle is less than in the 4:1 (by a factor $\sim$2), so that bodies trapped in the 4:1 have more time to evaporate before reaching the minimum periastron value (and $\nu = 180°$). For these reasons, it was not possible to get bodies that reach their minimum periastron value in the 4:1 simulations before being fully evaporated, where some bodies do it in the 3:1 simulations.

3. The role of the other orbital parameters

The simulations presented above have highlighted the crucial role of the eccentricity of the perturber's orbit for the efficiency of the 3:1 resonance. It is now worth wondering how these results are affected if we let the other parameters of the perturber evolve. Basically, this concerns its mass and its orbital semi-major axis. The role of the longitude of periastron has already been described as constraining the range of spectral velocities which FEBs events are to be expected.

In BM96, it was stressed that the semi-major axis a' on the planet orbit and its mass ratio μ with respect to the star are difficult to constrain just on the basis of FEB statistics, as the dynamic of FEBs depends only "weakly" on those parameters. As noted in BM96 and BM00, μ actually affects the width in the semi-major axis of the resonant zones, but weakly (it scales as $\sqrt{\mu}$). For larger μ values, we expect larger resonance zones, and thus more potential FEBs for the same population of bodies. μ also affects t_{FEB}, i.e., the characteristic time for eccentricity

Table 1. Output of simulations similar to those of Sect. 2, but for different mass ratios μ between the planet and the star. In each run, the particles are chosen with initial eccentricities between 0 and 0.1, and inclinations between 0 and 3°. Their semi-major axis are chosen between the limits $a_{\min}$ and $a_{\max}$ listed below, which correspond to the exact limits of the resonance zone at $e = 0.1$. In each case, the number $N_{\rm num}$ of particles simulated is fixed in order to keep a constant density of 2×10^6 particles per AU. For each run, the efficiency f is computed as the proportion of particles that have entered the dust evaporation zone ($q < 0.4$ AU) before $1\,t_{\rm coll}$ (5×10^5 yr). The characteristic time $t_{\rm FEB}$ is computed as the time of the main events peak (see Fig. 3), and $F_{\rm peak}$ is the observed peak frequency (number of events per 100 years). For all runs, the orbital parameters of the perturber are $a' = 10$ AU and $e' = 0.1$, and $\varpi' = -70°$ in the 4:1 case and $-50°$ in the 3:1 case.

μ	$a_{\min}$ (AU)	$a_{\max}$ (AU)	$N_{\rm num}$	f	$t_{\rm FEB}$ (yr)	$F_{\rm peak}$
4:1 case						
0.0002	3.96707	3.9696	5097	0.15	6.5×10^5	1500
0.0005	3.96609	3.9701	8067	0.185	2.7×10^5	3800
0.0007	3.96557	3.9703	9554	0.2	2.0×10^5	5000
0.001	3.96486	3.9706	11 428	0.2	1.4×10^5	6200
0.002	3.96288	3.9710	16 219	0.23	0.7×10^5	10 700
0.005	3.95811	3.9711	25 905	0.32	0.3×10^5	15 700
3:1 case						
0.0002	4.79961	4.81644	25 244	0.036	3.5×10^5	1700
0.0005	4.79550	4.82212	39 944	0.051	1.45×10^5	4800
0.0007	4.79358	4.82510	47 286	0.074	1.0×10^5	8000
0.001	4.79128	4.82899	56 557	0.10	0.77×10^5	11 000
0.002	4.78593	4.83952	80 372	0.18	0.36×10^5	28 000
0.005	4.77185	4.86344	137 376	0.53	0.14×10^5	85 000

growth: we have $t_{\rm FEB} \propto 1/\mu$, because the Hamiltonian is $\propto \mu$, and that for different (still small) values of μ it shares the same topology. Hence with different $t_{\rm FEB}$ values, the collisional equilibrium (see below) should be affected via Eq. (4). The mass of the planet finally may affect the efficiency f of the FEB generation mechanism. For a larger μ we expect a larger f.

The effect of changing the mass of the planet is illustrated in Table 1, which gives the basic result of several runs identical to those described in Fig. 3, but where we let μ vary. In each case, the number of particles computed is adapted to the width of the resonance in order to keep a numerical density of 2×10^6 particles per AU. The strength of the FEB mechanism is characterized by the efficiency f and the frequency of events at peak. Obviously, larger planetary masses trigger more efficiently a FEB phenomenon. As expected, the characteristic time $t_{\rm FEB}$ scales exactly as $1/\mu$. In both resonance cases, the efficiency appears roughly proportional to μ, while the peak frequency $F_{\rm peak}$ scales approximately as $\mu^{0.73}$ in the 4:1 case and as $\mu^{1.22}$ in the 3:1 case. It is worth noticing that the enhancement of the FEB phenomenon due to an increasing planetary mass is larger in the 3:1 case.

Similarly, we can investigate the role of the semi-major axis of the planet a'. Basically, for a similar population we expect a weaker FEB phenomenon for a larger a'. First, all time-scales should scale as the orbital periods, and thus scale as $a'^{3/2}$; second, when evolving towards large eccentricities under the effect of a resonance, the bodies keep their semi-major axis roughly unchanged, apart from a small amplitude secular libration. The location of the resonances scales obviously as a', as does the mean semi-major axis of the FEB candidates. Conversely, the location of the dust evaporation zone around β Pic, i.e., the periastron value they need to reach for generating spectral events, does not change. Hence, for a larger a', the FEB candidates need on average to get higher eccentricity values in order to generate spectral events. Fewer particles are thus expected to fit this more constraining criterion.

Table 2. Output of simulations similar to those of Sect. 2, but for different values of the planetary semi-major axis a'. The mass ratio between the planet and the star is fixed to $\mu = 0.001$. The conventions are the same as in Table 1. In both resonance cases, the number of particles simulated is kept constant irrespective of the value of a', and equal to the corresponding value listed in Table 1 for $\mu = 0.001$.

	4:1 case			**3:1 case**		
a' (AU)	f	$t_{\rm FEB}$ (yr)	$F_{\rm peak}$	f	$t_{\rm FEB}$ (yr)	$F_{\rm peak}$
10	0.2	1.4×10^5	6200	0.1	0.77×10^5	11 000
20	0.15	4.0×10^5	1800	0.095	2.1×10^5	1900
40	0.14	11.5×10^5	400	0.076	6.5×10^5	200

This effect is illustrated in Table 2, which describes, as does Table 1, runs similar to those of Fig. 3, but where now we let a' vary. In each case, we keep the number of particles simulated equal to the corresponding value in the runs of Fig. 3. Note that this is implicitly equivalent to considering a local body density in the resonance $\propto 1/a'$, as the width of the resonance scales as a'.

We see in Table 2 that increasing a' drastically affects the FEB phenomenon. In any case, the time $t_{\rm FEB}$ scales as $a'^{3/2}$ as expected. In the 4:1 case, the peak frequency $F_{\rm peak}$ appears to drop as a'^{-2}, while in the 3:1 case it drops even more steeply. If in each run we had adjusted the number of particles we simulate to the width of the resonance in order to keep the local density of bodies unchanged, then we would have $F_{\rm peak} \propto a^{-1}$ in the 4:1 case. The realistic picture lies perhaps between these two extremes. Weidenschilling (1977) derived a primitive surface density scaling as $r^{-3/2}$ in the primitive Solar nebula, and so a linear mass density $\propto r^{-1/2}$. With this scaling law, we should now expect $F_{\rm peak} \propto a^{-3/2}$ in the 4:1 case and an even steeper decrease in the 3:1 case. This means basically that doubling a' leads to decreasing the FEB activity by a factor 3 at least (a factor 10 if we multiply a' by 4). In such cases, the local density of bodies in the resonance would then have to be significantly larger if we want to make it account for the observed rate of FEB infall towards β Pic. This is the reason why we think that the perturbing planet

cannot orbit the star too far away from it. Of course the 10 AU value we assume is purely arbitrary, and we cannot constrain it better than by a factor of 2, but it seems to be a convenient typical value.

Even if larger a' values could not be excluded merely on this basis, a second dynamical constraint makes it difficult to imagine large a' values. When the FEBs are at high eccentricity, their periastron is very small, but their apoastron is close to $\sim 2a$ if a is their semi-major axis. Hence the FEBs virtually travel across all the disk located inside the orbit of the perturbing planet. If other planets orbit the star closer than the one we are considering, we should expect FEBs to undergo some close encounters with them, with possible ejection from the resonance and thus from the FEB process. In BM00, simulations were made assuming the presence of an Earth-sized planet orbiting the star well inside the orbit of the main perturbing planet. They showed that a significant number of bodies were affected, but this did not remove the FEB phenomenon, basically because the planet was small. Moreover, some of the bodies that were diverted from their resonant evolution by the terrestrial planet appeared to still approach the star with another orientation and possibly account for the blueshifted spectral events sometimes observed.

We made similar simulations, assuming now larger planets instead of the Earth-sized one. Inner large planets, even down to Uranus-sized planets, turn out to completely remove the FEB process, almost all bodies undergoing an encounter with the secondary planet. Therefore, an additional requirement of the model is that the planet responsible for the FEB phenomenon via its inner mean-motion resonances must be the innermost giant one. Conversely, outer planets (giant or not) are not excluded, as shown in BM00. Now, if we scale our knowledge of the Solar System to the β Pic case, even if we take into account that β Pic is significantly brighter than the Sun, assuming an innermost giant planet orbiting the star at more than 20 AU seems less realistic than at 10 AU.

4. Mutual collisions and resonance refilling

4.1. The need for a numerical approach

In BM00, the efficiency of mutual collisions among a population of bodies as a candidate for the refilling of the resonance was analytically estimated. Basically, the argument was the following: first, the local density of bodies *inside* the 4:1 resonance $N_{\rm in}$ was estimated to be $\sim 10^8$ bodies per AU, from the comparison between observed FEB frequency and results from numerical simulations such as those presented above. Then, a $N_{\rm out}/N_{\rm in} \simeq 5$ density ratio at collisional equilibrium was derived, where $N_{\rm out}$ is the linear density of bodies *outside* the resonance. Using then a classical Dohnanyi (1969) size distribution $\mathrm{d}N(r) \propto r^{-3.5}\,\mathrm{d}r$, this led to finally estimate the linear mass density of bodies within the disk to the range between a few and a few tens of Earth masses per AU. Such values are still realistic, but somewhat high. The last part of the calculation is nevertheless very poorly constrained, as it depends highly on the minimum size $R_{\rm FEB}$ we assume for the FEBs (15 km in the present case).

This showed nevertheless that mutual collisions are a possible mechanism for refilling the resonances that may generate FEBs. Such order of magnitude equilibrium calculations can however not fully take into account the complex behavior of a highly perturbed collisional system. As an example, they cannot estimate the concurrent "killing" effect that collisions might have on the FEB generating mechanism by extracting numerous highly eccentric bodies from the resonant regions. In order to more quantitatively estimate the refilling and killing effects, numerical simulations are clearly required. These simulations could not be performed until now because of too strong incompatible numerical constraints. Indeed, such simulations cannot be restricted to a population of bodies taken inside the FEB-generating resonance like the one presented above; taking into account the resonances themselves and their collisional reservoir, i.e., the adjacent regions to them, is even not sufficient. In fact bodies initially taken in a very large region extending over several AUs have to be considered, as FEB candidates may collide with all of them when their eccentricity grows.

At the same time the simulation must follow a statistically significant number of bodies actually trapped if the resonances if we want to derive valuable statistical properties. The resonances are very narrow regions on the semi-major axis ($\sim 10^{-3}$ AU for the 4:1), so that simulating a uniform population of bodies spread over several AUs while keeping a reasonable number of bodies inside the resonances forces us to consider number of particles in the computation which exceeds by far the present computing possibilities. Nevertheless, the situation is significantly improved if we focus on the 3:1 resonance as a major FEB source. As its width is $\sim 2.5 \times 10^{-2}$ AU, the required total number of bodies becomes more reasonable, though still relatively large, so that numerical tests might be performed.

4.2. The model

We will here use an adapted version of a model that was initially developed for the study of proto-Jupiter's perturbations on the early inner planetesimal disk (Thébault & Brahic 1999). It is worth recalling here briefly that this model follows, in a deterministic way, the evolution of a 3-D collisional system of $N_{\rm num}$ test particles, considered as indestructible spheres, submitted to external gravitational perturbations. The algorithm makes use of the fact that orbits are always close to Keplerian ones: it solves Kepler's equations for the central potential and it treats the perturbing potential by integrating Gauss' perturbing equations. All collisions are treated individually and collision outcomes are parametered by two transverse and tangential rebound coefficients $k_{\rm r}$ and $k_{\rm t}$. Mutual gravitational interactions are not taken into account, but this

assumption is fully justified for highly perturbed systems where encounter velocities significantly exceed individual escape velocities. We are not interested here in modeling a realistic physical outcome of high velocities impacts. Such impacts might result in catastrophic fragmentations, producing numerous fragments following complex size distribution laws, and are impossible to simulate with a deterministic simulation. The purpose of the present model is more to get an approximate estimate of the dynamical behavior of the collisional system by evaluating the dynamical effect of a collision, i.e., orbital modifications due to relative velocity exchange and energy loss, without following all the produced fragments. The same approach was also chosen, using a similar collisional model, by Marzari & Scholl (2000) for the study of planetesimal disks in close binary systems.

4.3. The choice of the parameters

The crucial parameter for such a collisional model is the optical depth, or total geometric cross section, of the system. Indeed, it can be shown that the collisional evolution of the "real" and numerical disks are equivalent for equal optical depths, i.e., for equal collision rates (Marzari & Scholl 2000).

Now, what is the expected optical depth for the β Pictoris planetesimal disk? A possible answer to this question could be given by the FEB simulations themselves, as they provide an indication on the expected number density of bodies bigger than a given size $R_{\rm FEB}$ (15 km). It has been shown (see Sect. 2.3) that the 3:1 resonance could sustain, during a few 10^5 years, a FEB activity requiring a 10^8 to 10^9 AU^{-1} body density in the real disk. As we expect that collision should enhance the long term FEB activity by refilling the resonance, we will assume as our reference value for the "real" disk the lower limit of this range, i.e., $N = 10^8$ AU^{-1}. This density value has to be completed by a size distribution estimate. Taking the equilibrium distribution assumed by BM00, i.e., $\mathrm{d}N(r) \propto r^{-3.5}\mathrm{d}r$ extending from $R_{\rm FEB}$ up to a $R_{\rm max} = 500$ km, the total geometrical cross-section per AU of the system reads:

$$\sigma = \int_{R_{\rm FEB}}^{R_{\rm max}} C\pi r^2 r^{-3.5}\,\mathrm{d}r = 2C\pi\left(R_{\rm FEB}^{-0.5} - R_{\rm max}^{-0.5}\right), \qquad (1)$$

where C is a normalization constant given by

$$C = \frac{2.5N}{R_{\rm FEB}^{-2.5} - R_{\rm max}^{-2.5}}. \qquad (2)$$

As a consequence, our choice of parameters for the numerical system must satisfy

$$\pi N_{\rm num} R_{\rm num}^2 = \sigma, \qquad (3)$$

where $N_{\rm num}$ is the linear density of particles in the disk actually integrated, and $R_{\rm num}$ their assumed fixed radius.

There are strong numerical constraints on $N_{\rm num}$ though, as the integration time crucially depends on this parameter. For a typical run extending over 10^6 yr, the maximum "reasonable" number of particles integrated (corresponding to 30 days of CPU time) is approximately 20 000. Thus, if we consider a disk extending from 0 to 10 AU, it follows that $N_{\rm num} \simeq 2000$ AU^{-1}. Unfortunately, this density is too low to provide enough bodies inside the 3:1 resonance in order to get enough FEB events. We will thus restrict our initial disk to a narrower region, and take $a_{\rm min} = 3.4$ AU and $a_{\rm max} = 6.6$ AU, i.e. $N_{\rm num} = 6250$ AU^{-1}. This assumption does not have any consequences for the collisional refill of the resonance, as it depends only on the regions immediately adjacent to the resonance, but might affect the collision statistics on those resonant bodies which undergo an eccentricity increase, as their aphelia and perihelia may reach regions that are artificially empty. Nevertheless, test simulations show that the error on the resonance collisional emptying rate does not exceed 10%, a rather reasonable value for the precision of our study. This is mainly due to the fact that the 6.6 to 10 AU region is highly dynamically unstable, and thus appears strongly depleted after a short time, for a planet with $\mu = 0.001$ and $e' = 0.1$, located at $a' = 10$ AU. The 10% are indeed due to particles orbiting the star inside 3.4 AU. This limited impact is due to the fact that the high eccentricity resonant bodies spend most of their time close to aphelion, i.e., outside this region.

With this value of $N_{\rm num}$, it follows from Eq. (3) that $R_{\rm num} = 3800$ km. The collision outcome parameters, $k_{\rm r}$ and $k_{\rm t}$, are chosen equal to -0.3 and 1 respectively. This corresponds to a radial energy dissipation of $\sim 90\%$, which is the usual value taken for high velocities impact (Petit & Farinella 1993). The global energy dissipation, when including the tangent non-dissipative component, is of the order of 50%. All the initial parameters for the simulation are summarized in Table 3.

Table 3. Initial parameters of the collisional simulation.

Number of bodies	20 000
Numerical radius of bodies	3800 km $= 2.5 \times 10^{-5}$ AU
Initial semi-major axis limits	3.4–6.6 AU
Initial eccentricity limits	0–0.1
Initial inclination limits	0–0.05 radians
Collisional parameters	$k_{\rm r} = -0.3$, $k_{\rm t} = 1$
Dust evaporation limit	0.4 AU
Planet mass / Stellar mass	0.001
Planet semi-major axis	$a' = 10$ AU
Planet eccentricity	$e' = 0.1$

4.4. Results

The results for a typical collisional run are presented in Figs. 6 and 7. Note that the 6250 AU^{-1} particle density that is imposed by the numerical constraints (see above) is too small to enable the same statistical analysis of the infall velocities as in the previous sections. Indeed, such a density corresponds to a factor 320 drop compared to the 50 000 bodies per 0.025 AU considered in the

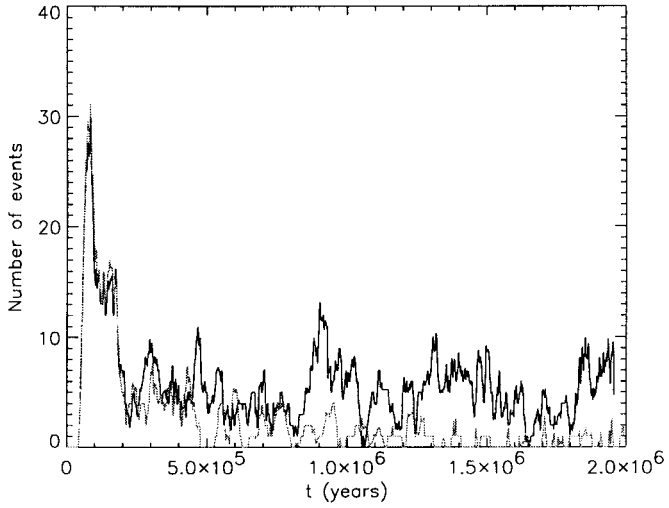

Fig. 6. Compared global evolution of the total FEB flux (with a 170 yr temporal bin) for the collisional run (dark line) and a template non-collisional case (grey line). Both runs start with the same initial conditions described in Table 3. The displayed number of events sums up the FEBs produced by the 3:1 and the 4:1 resonances. Evaporation in the FEB regime is taken into account for both simulations.

non-collisional runs of Sect. 2, but this is the price to pay for having a complete collisional simulation extending over several AUs. It is in particular difficult to keep here the strict definition of a FEB event, i.e., a body which actually crosses an imposed light of sight at less than 0.4 AU, because the final number of events would be much too small. We choose here to take an approximate and extended definition of a FEB event as being a body with a periastron value less than 0.4 AU, irrespective of its azimuthal orientation towards the line of sight. As the ratio of line-crossing versus total numbers of passages at $r < 0.4$ AU is approximately constant, the evolution of the "extended FEB events" parameter gives a reasonably good fit of the evolution of the exact number of events, as could easily be demonstrated by test simulations for the non-collisional runs. Nevertheless, the event statistics remains poor and is responsible for the relatively large fluctuations in the event frequency displayed in Fig. 6. Figure 6 displays the histogram of extended FEB flux over the 2×10^6 yr integration. For comparison purposes, the result of a similar run, but without taking collisions into account, is superimposed. Figure 7 displays instantaneous snapshots of the location in (a, e) space of all particles simulated, with a specific distinction (color code) on particles that were initially placed inside the 3:1 and 4:1 resonances, and those which were initially not.

The first thing we note is that the global shape of the FEB flux curve (Fig. 6) is similar to those of the non-collisional runs of Figs. 1 and 3. This fact validates our approach of considering only "extended" FEBs events (which was not the case in Sect. 2), and also shows to a first approximation that collisions do not remove the FEB phenomenon, i.e., collisions with disk particles do not extract a significant amount of high eccentricity bodies from the resonance before they reach the FEB state.

A more refined analysis of Fig. 6 reveals that the effect of collisions on the FEB scenario does not remain identical throughout the simulation run, but evolves with time. Basically, it can divided into two parts: first, during the first 2×10^5 yr corresponding to the peak activity, the collisional run remains very close to the nominal one. There is a small deficit in events, actually due to the collisional ejection of some resonant bodies. During the brief peak activity phase, this ejection-emptying mechanism dominates the collisional refilling, itself almost negligible. This can be seen in the Fig. 7a snapshot, taken after 75 000 yr, where the 3:1 and 4:1 resonances are still almost entirely populated by first generation bodies (indicated as black dots) originating from these regions. Note that Fig. 7a also provides a clear illustration of the respective importance of the different resonances, as discussed in Sect. 2, with the 3:1 clearly more populated with potential FEBs than the 4:1. Note also the strong 5:2 resonance at 5.4 AU, but with particles whose eccentricities do not exceed 0.8. This result is not surprising and was already discussed in BM96. As a matter of fact, the 5:2 resonance generates a population of fairly high eccentricity bodies, but which do not reach the FEB state.

After this first period, the situation then gradually evolves. For the non-collisional run, we observe in Fig. 6 a more or less progressive decrease in the number of events, already described in Sect. 2, due to the emptying of the initial reservoir of potential FEBs. In the collisional case, such a long-term decrease is not observed (apart from large oscillations due to the poor statistics of the runs). After the post-peak activity drop, the number of events remains at a relatively high and constant level during the entire run. This in fact is a direct consequence of the collisional refill of the FEB-producing resonances. Indeed, the collisional incoming flux of bodies inside the resonances, which depends on the average density and dynamical conditions in the main swarm, remains at a constant level during all the run. The slow decrease of the initial FEBs reservoir, due to FEB consumption by evaporation, appears thus progressively compensated by new incoming objects. This shows up clearly in Fig. 7c, which shows that after 6×10^5 yr, almost none of the highly eccentric objects produced by the 3:1 resonance originate initially from this region.

Furthermore, the fresh bodies that get into the resonances thanks to collisions have in fact more chances to rapidly become FEBs than the bodies that were initially placed in the resonances. The reason for this is that collisionally injected bodies arrive with relatively higher eccentricities, typically ranging between 0.1 and 0.2, while initial particles were initially taken between $e = 0$ and $e = 0.1$. This is illustrated in Fig. 8, where the location of some of these collisionally injected particles in (a, e) space is displayed, showing an average eccentricity much larger than 0.1. The 3:1 resonance topography is obviously more favorable for FEB evolution for particles with $e = 0.2$

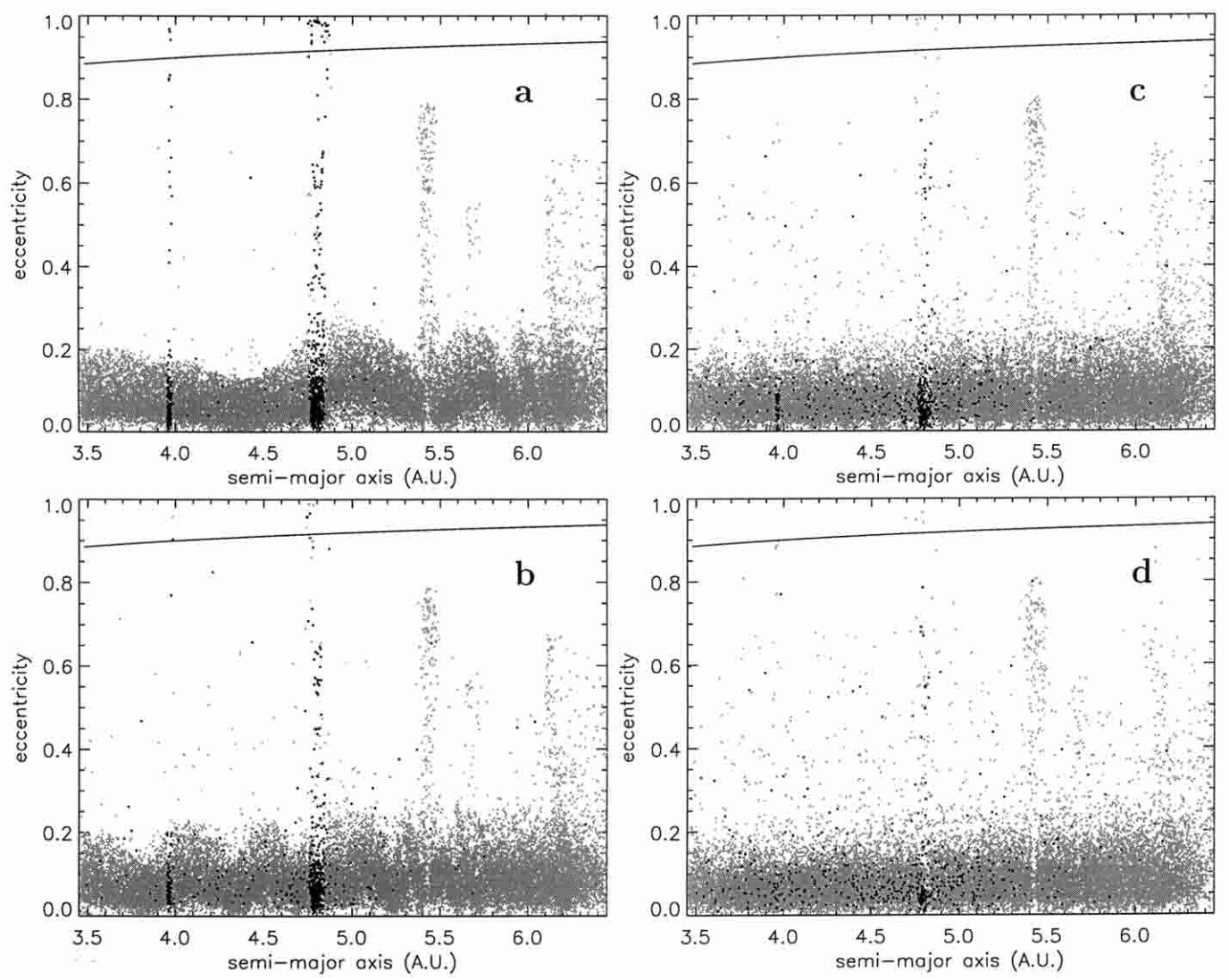

Fig. 7. Evolution snapshots of the whole collisional system in the (a, e) diagram after **a)** 75 000 yr, **b)** 3×10^5 yr, **c)** 6×10^5 yr and **d)** 2×10^6 yr. The black dots indicate the bodies that were *initially* placed in the 3:1 and in the 4:1 resonances, while grey dots indicate particles that were initially outside these resonances (but could be in other ones like the 5:2). The upper solid line marks the limit of the FEB regime: bodies above this limit have periastron values inside the dust evaporation region ($\sim$0.4 AU), and are therefore likely to be observed. The progressive spreading of the resonant bodies in the disk is a direct consequence of the collisions they suffer (see Thébault & Brahic 1999).

initially than with $e \leq 0.1$ (Fig. 2). Moreover, the resonance is wider in the semi-major axis at $e = 0.2$ than at $e = 0.1$, so that resonant trapping of new bodies is expected to be easier at higher eccentricities.

Finally, after the first activity peak, the bodies initially placed inside the resonance, but that are still at low eccentricity, are on average bodies with large amplitude libration in their resonant motion, which are not very likely to initiate a FEB-like high-eccentricity cycle. Consequently, after a few 10^5 yr, all FEB events are due to bodies that were initially *not* in the resonance. The refilling mechanism is thus relatively powerful in terms of FEB production.

After the first peak period, the collisional FEB scenario becomes in fact fully decoupled from the non-collisional one, as the long-term activity decrease appears efficiently compensated by the injection of fresh bodies into the resonance. In other words, the time scale for refilling of the resonance is shorter than the time scale for the FEB activity decrease. It can be estimated that for the period lasting from 2×10^5 yr to 10^6 yr, the average number of events obtained in the collisional run exceeds by more than a

Table 4. Total number of bodies that have become FEBs 1) during the peak activity period and 2) after the end of the peak activity, for the collisional and non-collisional runs.

Number of FEBs	Non-collisional run	Collisional run
$0 < t < 2 \times 10^5$ yr	55	51
2×10^5 yr $< t < 2 \times 10^6$ yr	52	108
Total	107	158

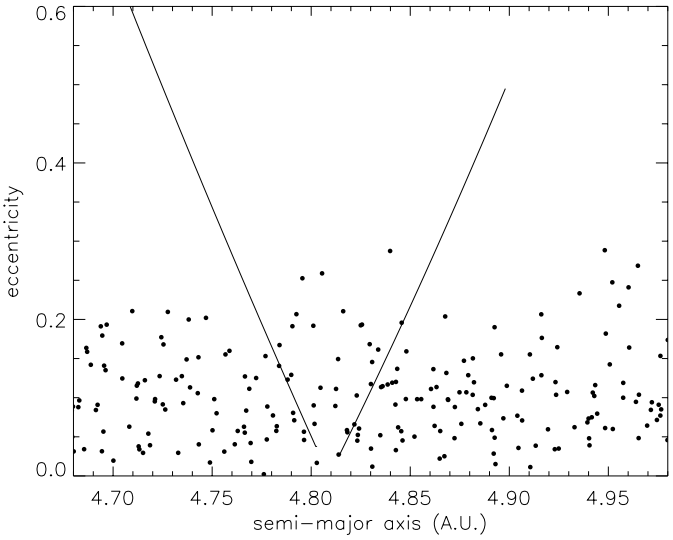

Fig. 8. Positions, in (a, e) space, of the bodies having entered the 3:1 resonant area during the 5×10^5–6×10^5 yr time interval. The solid lines mark the border of the resonant region, as calculated by BM96.

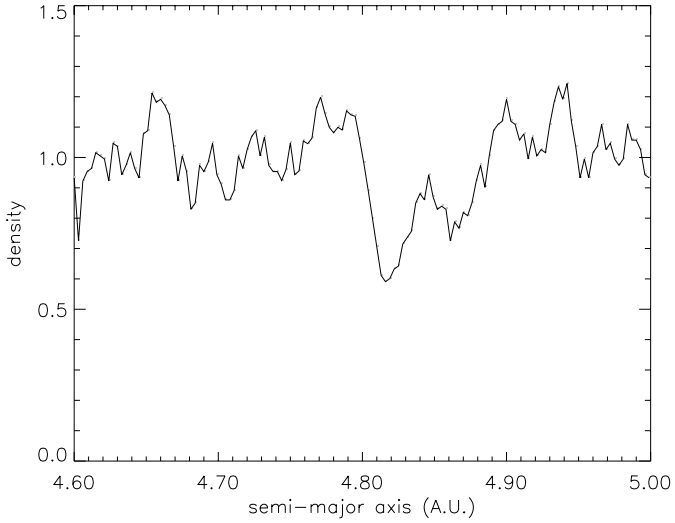

Fig. 9. Linear Density profile around the 3:1 resonance at $t = 10^6$ yr. The densities have been normalized to the average value outside the resonance.

factor of 2 the value obtained for a non-collisional run (see Table 4). Since for such a non-collisional run this activity requires a "real" disc of approximately 10^8–10^9 bodies per AU (see Sect. 2.3), it follows that, for the same period, a density of only half this value is required for the collisional case. There is of course an additional significant advantage here, i.e., this average value does not rise with time, since the FEB-producing level does not decrease as it does in the non-collisional case. It thus remains constant for the following 10^6 to 2×10^6 yr period.

For computing time sparing reasons, we did not carry on the integration further than 2×10^6 yr. Nevertheless, the average FEB level observed at $t = 2 \times 10^6$ yr might be, with rather good confidence, extrapolated to longer time scales. This is a consequence of the decoupling of the collisional and non-collisional runs, and in particular of the fact that after a few 10^5 yr it is the collisional refill of the resonances which takes over the generation of new FEBs. Thus, as long as the collisional incoming flux of bodies does not dry up, the steady-state regime the FEB activity reaches after 5×10^5 yr should keep on and might probably last for times greatly exceeding 2×10^6 yr.

Another important remark can be made concerning the density profile around the 3:1 resonance. Figure 9 shows the linear density profile of our numerical disk around the 3:1 resonance region at $t = 10^6$ yr, i.e., well into the steady-state regime. A density drop here is clearly observed at the location of the resonance, but it remains relatively moderate. The $N_{\rm out}/N_{\rm in}$ ratio between the outside and inside resonance densities is $\sim$1.5. This is significantly different to the $N_{\rm out}/N_{\rm in} = 5$ ratio estimated by BM00, but for the 4:1 resonance. BM00 used the simplified analytical formula

$$\frac{N_{\rm out}}{N_{\rm in}} = 1 + f\frac{t_{\rm coll}}{t_{\rm FEB}}, \qquad (4)$$

where $t_{\rm coll}$ and $t_{\rm FEB}$ are respectively the collision time-scale and the FEB evolution time-scale, i.e. the typical time-scale for resonance eccentricity increase. For both resonances $t_{\rm FEB}$ is roughly 10^5 yr. BM00 assumed $t_{\rm coll} = 10t_{\rm FEB} = 10^6$ yr, and $f = 0.4$. It is possible here to derive from our collisional run a more accurate estimate of $t_{\rm coll}$, namely $t_{\rm coll} \simeq 5 \times 10^5$ yr (the time after which non-resonant and resonant runs are fully decoupled). The value of f for the 3:1 resonance was already estimated in Sect. 2 to $\sim$0.1. With these values Eq. (4) yields $N_{\rm out}/N_{\rm in} = 1.65$, which is remarkably close to the numerical value (1.5) obtained from the simulations. This in fact validates the simplified approach as a first investigation tool of the role of collisions.

4.5. Higher collision rate

Because our algorithm is very computing-time-consuming, we could not explore all the free parameters for our collisional model. Nevertheless, we did perform one additional run with a higher collision rate, i.e., with larger numerical test particles, in order to test the robustness of the presented results towards this crucial parameter. Figure 10 presents the FEB flux obtained for a disk having an optical depth 20 times higher than in the nominal case, i.e., with $R_{\rm num} = 17\,000$ km, or an average collision time scale of approximately $t_{\rm coll} = 40\,000$ yr. This is clearly an extreme case, since such a high optical depth corresponds to a highly unrealistic very massive physical disk.

The obvious difference with the previous results is the total absence of the early high activity peak. This is because the collision time scale of the resonance-trapped bodies is shorter than $t_{\rm FEB}$. Thus, after $t = 8 \times 10^4$ yr, i.e. the approximate moment when the peak activity should be reached (see Fig. 6), there are almost no high eccentricity objects in the 3:1 resonance which were initially located there. This is clearly illustrated in Fig. 11, which shows

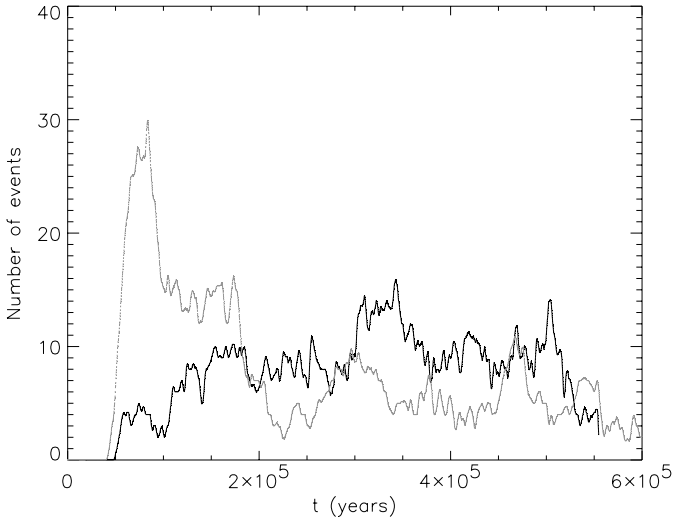

Fig. 10. Same as Fig. 6, but for a higher collision rate, i.e., with $R_{\rm num} = 17\,000$ km (black line). The grey line corresponds to the collisional run displayed in Fig. 6.

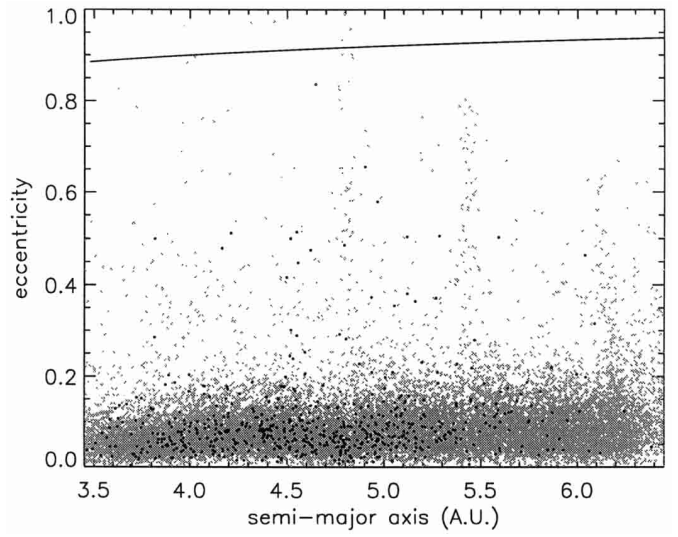

Fig. 11. Snapshot similar to those presented in Fig. 7, but for the high collision rate run, after only 10^5 yr. The plotting conventions are the same as in Fig. 7.

that after 10^5 yr all the initial resonant particles have been spread out in the system and that the resonances have been refilled with new objects. In other words, this means that at this epoch, the evolution of the collisional system is already completely decoupled from that of the non-collisional one, this decoupling happening much earlier than for the nominal collisional run. As a consequence, there is no peak activity due to initial resonant bodies to be observed. The system thus quickly reaches a stationary regime dominated by the collisional emptying and refilling of the resonances. Surprisingly enough, the average FEB activity in this regime is comparable, if not superior, to that observed for the nominal run. Indeed, one could expect a lower activity due to the rapid ejection of all high-eccentricity bodies from the resonances. But this high outgoing flux of bodies is compensated by a higher incoming

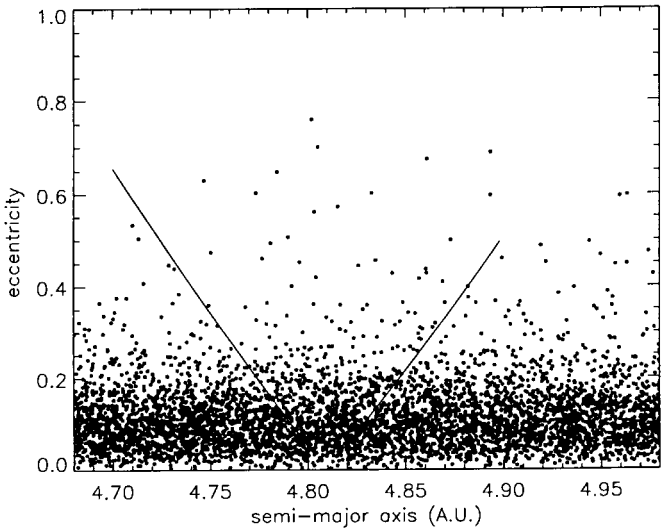

Fig. 12. Same as Fig. 8 (location of particles that entered 3:1 resonance between 10^5 and 1.5×10^5 yr), but for the high collision rate run.

flux of objects, the main reason being that these incoming particles have very high eccentricities when entering the resonant area (see Fig. 12), much more than in the nominal case (Fig. 8). The collision rate is so high that large high-eccentricity sources like the 5:2 resonance at 5.4 AU continuously feed the swarm, including the 3:1 resonant area, with high-eccentricity particles. These high e incoming objects are very good FEB candidates and might reach the FEB zone limit in relatively short time. One should also note that there are now a few FEB objects which are not trapped inside the 4:1 or 3:1 resonances (see Fig. 11). These particles have reached the FEB limit directly after a violent impact between one or two high eccentricity objects. These additional events probably reach the FEB state with different periastron orientation and might contribute to the low flux of blueshifted events.

As a consequence, the global FEB activity of the collisional stationary regime remains at a high level. The results discussed earlier in the present section are thus remarkably insensitive to the collision rate in the disk. Contrary to what could be expected there is no tendency for collisions to "destroy" the FEB-producing mechanism. Of course, this destruction effect should appear for very high collision rate, but these rates will greatly exceed the already too large and unrealistic one considered here. We might thus conclude with rather good confidence that the presented results are relatively generic, at least concerning the optical depth/collision time scale parameter.

4.6. Effect of collisional erosion

It is clear that our academic model cannot be taken as an exact representation of the behavior of a "real" system of planetesimals impacting at high velocities. In the "real" disc, we expect bodies to be fragmented after several violent impacts. It is in particular likely that after numerous successive impacts, the size of the remaining

bodies will progressively decrease and will lie well below the FEB size limit $R_{\rm FEB}$, thus strongly lowering the number of FEB events. Nevertheless, it should be noted that in our nominal run, we are far from being in this case of multiple successive collisions, since the average number of collisions suffered by a body by the time it enters (after an impact) a FEB producing resonance is only 1.5. Thus, most of the bodies entering the resonant FEB-producing areas are first-generation collisional products. If we suppose that our test particles stand for the biggest impact-produced fragments, then these fragments would have a size of approximately 1/4 that of the initially impacting objects (considering typical 500 $\mathrm{m\,s^{-1}}$ impacts and the biggest fragment size empirical law as considered e.g. by Petit & Farinella 1993). With impacting objects of typically 30 km, this will lead to ∼7–8 km fragments, which, though significantly smaller, still remain in the same size range. Considering the large uncertainties on the $R_{\rm FEB}$ limit, these fragments might thus still be considered as potential FEB candidates. Moreover, it should be reminded that theoretically *any* body is a potential FEB candidate, regardless of its size. Differences in sizes only lead to different durations of the FEB phase before evaporation. $R_{\rm FEB}$ gives only an indication of the size for which the FEB episode lasts a "reasonable" time. We could try to be more "realistic" by shortening the FEB duration of bodies which have suffered a violent collision. But this would not be a satisfying solution, as in the "real" disk, this shorter FEB duration of every produced fragment would probably be compensated by the fact that each collisions produces not only one, but several large fragments, which cannot all be taken into account in our deterministic model.

The multiple collision erosion effect might be more important for the higher collision rate case, where the average number of collisions per particle is 8.5 after 10^6 yr. But anyway, as already mentioned, this case is rather academic, since it requires highly unrealistic densities.

5. Discussion

As already mentioned, the numerical results concerning the FEB-generating mechanism might be very useful in the sense that they provide, under certain assumptions, some indirect information on the characteristics of two distinct populations of the β Pic system which are presently not accessible to observations, i.e., the kilometer-sized planetesimals and a hypothetical giant planet.

5.1. The planetesimal disk

5.1.1. Deriving disk population and mass estimates

In the previous sections, it has been shown that the coupled effect of an efficient 3:1 resonance and of mutual collisions is a powerful FEB generating mechanism able to last on long time-scales to allow the mechanism to be still active today.

Based on non-collisional simulations for the 4:1, BM00 derived disk population and mass estimates. It is now worth trying to do the same using the results of our collisional run, and on the basis of the *steady-state* regime that applies after $\sim 3\times10^5$ yr instead of the activity peak at $\sim 10^5$ yr.

To make these estimates, we must return to the non-collisional runs of Sect. 2, because the statistics of FEB events for these runs were made using a well-defined line of sight, which was not the case in the collisional run. In Fig. 3, we see that the peak activity for the 3:1 resonance is $F_{\rm peak} \sim 11\,000$ events per 100 years. Now, Fig. 6 shows that in the collisional situation the ratio of pseudo-FEB events between the activity peak and the subsequent steady-state regime is ∼5 (we shall call this ratio δ). Therefore, if we had been able to perform a collisional run with as many particles initially in the 3:1 resonance as in Sect. 2, we would expect to have a steady-state regime with $F_{\rm num} \sim 2200$ events per 100 years.

The real average FEB activity towards β Pic can be estimated as $F_{\rm obs} = 1000$ events per year (BM00) (or 10^5 events per 100 yr). We expect the real population in the resonance to be in a ratio $F_{\rm obs}/F_{\rm num}$ with respect to the simulated one. We then derive the local density in the resonance $N_{\rm in}$ as

$$N_{\rm in} = \frac{F_{\rm obs}}{F_{\rm num}}\Lambda = \delta\frac{F_{\rm obs}}{F_{\rm peak}}\Lambda, \tag{5}$$

where $\Lambda = 2\times10^6$ $\mathrm{AU^{-1}}$ is the fixed numerical density in the simulations of Sect. 2.

This yields $N_{\rm in} \simeq 9.1\times10^7$ $\mathrm{AU^{-1}}$. Now using Eq. (4) with $f = 0.1$ and $t_{\rm coll} = 5\times10^5$ yr, we derive $N_{\rm out} \simeq 1.5\times10^8\,\mathrm{AU^{-1}}$. Assuming the BM00 size distribution ($r^{-3.5}$ differential size law), the linear mass density $M_{\rm plan}$ of planetesimals may be derived as

$$M_{\rm plan} = \frac{20}{3}\pi N_{\rm out} R_{\rm FEB}^3 \rho \left(\sqrt{\frac{R_{\rm max}}{R_{\rm FEB}}} - 1\right), \tag{6}$$

where ρ is the density of the solid body. With $\rho = 1\ \mathrm{g\,cm^{-3}}$, $R_{\rm FEB} = 15$ km and $R_{\rm max} = 500$ km, we derive $M_{\rm plan} \simeq 8.5\,M_\oplus$ of planetesimals per AU.

Note that this value is self-consistent with that assumed to estimate the collision rate, which makes the simulation self-coherent.

Of course, the same can be done on the results of all the runs described in Sect. 3, where we let a' and μ vary. We made other collisional simulations corresponding to each case in order to estimate how the peak/plateau ratio δ varies. The result is displayed in Table 5. The first observation we can note is that as expected, if the planet orbits the star too far away from it, then the disk population we deduce is unrealistic. For such a planet, the FEB generation mechanism is not very efficient, so that in order to account for the observed rate, a truly huge population would be required. From these results, we may stress that the upper acceptable limit for a' is ∼20 AU.

Table 5. Disk populations ($N_{\rm in}$, $N_{\rm out}$) and linear mass densities ($M_{\rm plan}$) that can be deduced from the outputs of the runs of Sect. 3. In each case, the ratio δ between the peak 3:1 activity and the collisionally sustained activity level was derived from a dedicated collisional simulation like the one presented in Fig. 6 for $\mu = 0.001$ and $a' = 10$ AU.

Run conditions	δ	$N_{\rm in}$ (3:1) ($\rm AU^{-1}$)	$N_{\rm out}$ ($\rm AU^{-1}$)	$M_{\rm plan}$ ($M_\oplus\,\rm AU^{-1}$)
($\mu = 0.0002, a' = 10$ AU)	2	2.35×10^8	2.47×10^8	14.0
($\mu = 0.0005, a' = 10$ AU)	1.5	6.25×10^7	7.35×10^7	4.1
($\mu = 0.0007, a' = 10$ AU)	2	5.00×10^7	6.85×10^7	3.9
($\mu = 0.001, a' = 10$ AU)	5	9.09×10^7	1.50×10^8	8.5
($\mu = 0.002, a' = 10$ AU)	6	4.29×10^7	1.50×10^8	8.5
($\mu = 0.005, a' = 10$ AU)	9	2.12×10^7	4.22×10^8	23.8
($\mu = 0.001, a' = 20$ AU)	5	2.63×10^8	4.25×10^8	24.0
($\mu = 0.001, a' = 40$ AU)	5	1.25×10^9	1.87×10^9	105.3

Second, we note that if we let the planetary mass vary, then the disk population we derive (and so the mass estimate) does not vary monotonously with μ; there seems indeed to be an optimum around $\mu = 0.0005$–0.001. This may be explained as follows: for small planetary masses, the FEB generation mechanism is not very powerful (small f), the time for eccentricity increase ($t_{\rm FEB}$) is long, and the resonances are very narrow. Requiring the observed rate to be replicated by such a model requires a very crowded disk. Conversely, if the mass of the planet is high (typically $\mu = 0.005$ and above), then the mechanism is very powerful, and $t_{\rm FEB}$ is so short that the collisions barely succeed in refilling the resonances. Consequently, a high population *outside* the resonances ($N_{\rm out}$) is required to sustain the activity.

Finally, planetary masses around $\mu = 0.0005$–0.002 ($\sim$1 to 4 Jupiter masses) seem to be best able to account for the FEB mechanism with a reasonable disk population.

5.1.2. Limitations to this approach

These results must be taken with care, as many numerical parameters used to derive these values are only poorly constrained. Nevertheless, we may trust the inside populations $N_{\rm in}$ we obtain. Deriving $N_{\rm out}$ from $N_{\rm in}$ is done via Eq. (4). Although $t_{\rm coll}$ is rather weakly constrained, the analysis of Fig. 9 shows that we may be confident in the use of this equation, so that we may also trust the $N_{\rm out}$ values we derive. Conversely, obtaining $M_{\rm plan}$ from Eq. (6) requires the use of parameters that are very badly constrained.

The first one is the value of $R_{\rm FEB}$. In the present paper and in BM00, it was assumed that $R_{\rm FEB} = 15$ km, but this parameter actually critically depends on the evaporating process assumed for the FEBs. A given FEB crossing the line of sight closer to the evaporation limit of refractory material may be observed in absorption only if it can develop around it a large and dense enough coma of metallic material. The coma needs to be large in order to mask a significant fraction of the stellar surface, and it also needs to be dense enough to be optically thick in the spectral lines observed. Note that *both* conditions are required. Basically, these conditions are fulfilled if the FEB evaporates at a high enough rate. Previous studies (see e.g. Beust et al. 1996) have shown that the required rates are typically $\sim 3 \times 10^7$ $\rm kg\,s^{-1}$ within one order of magnitude. At this evaporation rate, $R_{\rm FEB} = 15$ km is the typical size of bodies which are able resist a large enough number of periastron passages within the dust evaporation limit ($\sim$0.4 AU) to see their periastron distance significantly decrease below this limit under the resonant dynamic (BM00). 1 km-sized bodies typically evaporate within a few tens of periastron passages as soon as they get into the dust evaporation limit, so that i) they do not generate numerous events, and ii) their periastron value does not decrease much below the limit before they completely evaporate. Indeed, the presence of moderate to high velocity events requires periastron values significantly below the limit.

Furthermore, there is still a large uncertainty about the presence of volatiles in the FEB progenitors. In previous modeling (Beust et al. 1996), calculations were made assuming that volatiles (i.e., evaporated ices) are an important component of FEBs. Recently, however, some doubt about the presence of these volatiles has arisen, since at the stellar distances from which the FEBs are supposed to originate ($\sim$5–10 AU), ices might not survive the age of the system against sublimation, even embedded in a refractory matrix (Karmann et al. 2001). If volatiles are not present, then the dynamics of metallic ions in FEB coma should be affected, leading perhaps to a revision of the needed evaporation rate, and subsequently of $R_{\rm FEB}$. This modeling work is presently under way.

Another major point is the size distribution assumed above $R_{\rm FEB}$. The $\sim 10\ M_\oplus\,\rm AU^{-1}$ estimate of Table 5 was derived assuming an equilibrium differential law in $r^{-3.5}$ extending up to $R_{\rm max} = 500$ km. Such an assumption remains highly hypothetical and cannot be correlated to any direct or indirect observational evidence. This law is indeed the most reasonable one (and usually assumed) for a collisional system which has had enough time to reach equilibrium, but other size distribution $r^{-\alpha}$ might be possible, as collisionally-evolved systems such as the asteroid belt present clear departures from this theoretical law, although these departures remain limited. In this respect, it might be useful to express how Eq. (6) is modified with other power law distributions. The differential size probability function above $R_{\rm FEB}$ reads

$$p(r)\,{\rm d}r = \frac{\alpha - 1}{R_{\rm FEB}} \left(\frac{r}{R_{\rm FEB}} \right)^{-\alpha} {\rm d}r, \qquad (7)$$

and the linear mass density is computed as

$$M_{\rm plan} = \int_{R_{\rm FEB}}^{R_{\rm max}} N_{\rm out} p(r) \frac{4}{3} \pi \rho r^3 \, {\rm d}r = \frac{4}{3} \frac{\alpha - 1}{4 - \alpha} \pi \rho N_{\rm out} R_{\rm FEB}^3 \left[\left(\frac{R_{\rm max}}{R_{\rm FEB}} \right)^{4-\alpha} - 1 \right]. \quad (8)$$

When considering "reasonable" α values, typically ranging from 3.2 to 3.8, the size distribution has a rather limited influence, about an order of magnitude, on the total mass of large bodies. For the same range of α, changing the value of $R_{\rm max}$ has also limited consequences. The crucial parameter here is $R_{\rm FEB}$, as $M_{\rm plan}$ scales approximately with $R_{\rm FEB}^{\alpha-1}$. As a consequence one has to remain very careful when considering mass estimates deduced from disk population estimates. Nevertheless, it seems that, at least to a first approximation, the mass density estimate deduced falls within a range which is close to the expected mass density of planetesimals in the early Solar System. This value should not be extrapolated to estimate the total mass of the inner disc, as there could be a large fraction of this mass that might be contained in bigger, planetary or proto-planetary, objects. These objects are completely "invisible" to our study, since they almost do not contribute to the total optical depth, and thus to the FEB flux.

5.2. The perturbing planet

The major assumption behind any FEB-generating mechanism is the presence of a massive perturbing planet. In the present study, it has been shown that reaching a satisfying level of FEB production from a reasonably populated planetesimal disk requires a planet with a mass falling in the range 1 to 4 times that of Jupiter, orbiting the star at typically 10 AU (within a factor 2 uncertainty), with an orbital eccentricity around 0.1. How generic is such a assumption?

First of all, the presence of an already-formed massive planet seems compatible with the estimated age of the system (10^7–10^8 years). The standard models of gaseous giant formation predict formation time-scales typically one order of magnitude shorter than this range (see e.g. Pollack et al. 1996).

Moreover, and independent of the FEB phenomenon, there has been in recent years a growing suspicion that there may be planets orbiting β Pic, at least one Jupiter-like giant planet. Basically, such a planet was often invoked as responsible for the various asymmetries (Kalas & Jewitt 1995) observed between the two extensions of the dusty disk (see e.g. Lazzaro et al. 1994; Roques et al. 1994).

Lecavelier et al. (1995) analyzed archival photometric observations of β Pic and found unusual brightness variations that could be indirectly produced by a massive body embedded in the disk, but this hypothesis seems obsolete today. One of the most convincing arguments for the presence of a giant planet was presented by Mouillet et al. (1997), who explained the observation of a warp of the inner disk ($\lesssim$50–100 AU) with respect to the outer one (Burrows et al. 1995; Heap et al. 2000) by the presence of a planet on an inclined orbit. It should be noted that the characteristics of the proposed planet are compatible with the perturbing body considered in the present study, i.e., an object with a mass in the ratio 0.001 with that of the star, located at $\sim$10 AU from the star. As a matter of fact, Mouillet et al. (1997) and Heap et al. (2000), on the basis of the radial extension of the warp, of its time to progress further out, and of the estimated age of β Pic, came to the conclusion that the planet could not be located further out than 20 AU, which is exactly the conclusion we derive here independent of the FEB activity level.

Mouillet et al. (1997) nevertheless focused their study on the inclination of the perturbing planet and could not deduce strong constrains on its eccentricity. However, there seems to be a rather good convergence of different arguments that tend to indicate the presence of at least one Jupiter-like object with such orbital characteristics.

The major non-generic characteristic of our perturbing planet is its eccentricity. Taking $e' \simeq 0.1$ is obviously not a fully generic assumption, as this value lies above that of the Solar System planets. However, a significant number of extra-solar giant planets discovered recently by radial velocity measurements have eccentricities well above the 0.1 limit (see e.g. Gonzalez et al. 1999; Vogt et al. 2000).

Moreover, even if we consider the Solar System, 0.1 does not appear to be an unrealistic eccentricity value if we suppose the presence of other massive planets in the β Pic system. Let us here recall that due to their mutual interactions, Jupiter and Saturn have oscillating orbital elements which allow them to reach $e' = 0.06$ and 0.1 respectively. To reach $e' = 0.1$ for our Jovian perturbing planet, it is reasonable to assume the presence of another (external) body of at least comparable mass.

6. Conclusion: A possible coherent view of the β disk

The present work confirms that a giant planet on a slightly eccentric orbit could be the dynamical source for the flux of Falling Evaporating Bodies (FEBs) observed as transient absorption events in the β Pic spectrum. These bodies, which are believed to be at least kilometer-sized planetesimals, are produced by the 4:1 but mostly by the 3:1 resonances with the perturbing planet on a typical time scale of 10^5 years. The crucial point of sustaining this FEB activity for a time scale representing a non-negligible fraction of the star's age has also been addressed. Numerical simulations show that mutual collisions among planetesimals might be an efficient mechanism for refilling the FEB producing resonances at a satisfying rate. But other refilling mechanisms such as planetary migration cannot be completely ruled out.

One has to remain very careful concerning the previous analysis, since it relies on several hypothetical assumptions and on poorly known parameters. Nevertheless, this first analysis, compared to independent results concerning

the dust disk, tend to provide us with a rather coherent vision of the inner β Pic disk:

- A giant Jupiter-like planet orbits the star at a distance of 5 to 20 AU. $a' = 10$ AU is a typical likely value. The orbital eccentricity of this planet is $\sim$0.1. Its periastron is shifted by $\sim -70°$ with respect to the line of sight. This planet is responsible for the warp and for the FEB phenomenon.
- Inside the orbit of this planet, we find no other gaseous giant, but possibly terrestrial-like planets that may scatter some of the FEB candidates and produce the unusual blueshifted events (Crawford et al. 1998; BM00).
- Apart from these possible terrestrial planets, the disk inside the giant planet's orbit is basically a disk of planetesimals that continuously produce dust particles by collisions and evaporation. At specific locations that correspond to the major mean-motion resonances with the planet, the planetesimals are forced to evolve towards high eccentricities, which make them virtually cross all the disk inside the planet's orbit. Those which are trapped in the 4:1 and 3:1 resonance reach truly star-grazing orbits and may be observed as FEBs.
- These resonances are refilled by collisions among planetesimals from the population adjacent to the resonances. On a time-scale $\lesssim 10^8$ yr, we expect this process to dynamically sculpt the planetesimal disk, removing most of its mass by FEB evaporation, ejection out of the system by close encounters with the terrestrial planets, or collision with the terrestrial planets themselves (if present). Once this is achieved, the FEB process should stop and leave a planetesimal disk much like the present Solar asteroid belt.
- Outside the orbit of this planet, we find a dynamically less evolved, and less collisional (lower eccentricities) planetesimal disk that produces most of the dust observed in scattered light. The outside part of this disk ($r \gtrsim 80$ AU) is still in its primordial state, with a mid-plane tilted by a few degrees with respect to the orbit of the main planet. When they are smaller than 10 μm, the dust particles produced by all these planetesimals are pushed away by radiation pressure on highly elliptical or even hyperbolic orbits, and are visible up to $\sim$1000 AU. Poynting-Robertson drag is far weaker than radiation pressure and cannot prevent this ejection of dust.
- In response to the gravitational pull of the planet, the outer disk progressively assumes the same mid-plane as the planet's orbit. This readjustment progresses from inside to outside. The observational result is the observed warp which appears to be a transient feature: in the future, the whole system is expected to adopt the planet's orbital plane as mid-plane. At present the dust is produced by the warped population and the not warped one, which propagates the asymmetries of the disk outwards.
- The presence of additional giant planets orbiting the star outside the orbit of the main planet is hard to constrain: first, if other massive bodies are present (of mass comparable to the main planet), then we expect the "warp" to achieve a much more complex structure and perhaps disappear, as these additional planets will probably not have the same orbital plane as the main planet, and not the same line of nodes. Second, if no other planet is present, then the fairly high eccentricity of the main planet ($\sim$0.1) is harder to explain, as secular perturbations among the planets may cause this eccentricity to reach such values. Finally, Uranus-sized or even Saturn-sized bodies could be the best compromise.
- The recent passage of an M-dwarf might have perturbed the disk and generated the ring-like structures detected in the outermost part of the disk (500–800 AU; Kalas et al. 2000).

References

Artymowicz, P. 1997, Ann. Rev. Earth Planet. Sci., 25, 175

Bailey, M. E., Chambers, J. E., & Hahn, G. 1992, A&A, 257, 315

Barrado y Navascués, D., Stauffer, J. R., Song, I., & Caillault, J.-P. 1999, ApJ, 520, L123

Beust, H., Lagrange-Henri, A.-M., Vidal-Madjar, A., & Ferlet, R. 1990, A&A, 236, 202

Beust, H., & Morbidelli, A. 1996, Icarus, 120, 358 (BM96)

Beust, H., Lagrange, A.-M., Plazy, F., & Mouillet, D. 1996, A&A, 310, 181

Beust, H., Lagrange, A.-M., Crawford, I. A., et al. 1998, A&A, 338, 1015

Beust, H., & Morbidelli, A. 2000, Icarus, 143, 170 (BM00)

Beust, H., Karmann, C., & Lagrange, A.-M. 2001, A&A, 366, 945

Boggess, A., Bruhweiler, F. C., Grady, C. A., et al. 1991, ApJ, 377, L49

Burrows, C., Krist, J. E., & Stapelfeldt, K. R. 1995, BAAS, 187, #32.05

Brunini, A., & Benvenuto, O. G. 1996, MNRAS, 283, L84

Crawdord, I. A., Beust, H., & Lagrange, A.-M. 1998, MNRAS, 294, L31

Crifo, F., Vidal-Madjar, A., Lallement, R., Ferlet, R., & Gerbaldi, M. 1997, A&A, 320, L29

Dohnanyi, J. S. 1969, JGR, 74, 2531

Gonzalez, G., Wallerstein, G., & Saar, S. H. 1999, ApJ, 511, L111

Grady, C. A., Sitko, M. L., Bjorkman, K. S., et al. 1997, ApJ, 483, 449

Grady, C. A., Pérez, M. R., Bjorkman, K. S., & Massa, D. 1999, ApJ, 511, 925

Grady, C. A., Sitko, M. L., Russell, R. W., et al. 2000, Infalling Planetesimals in Pre-Main Sequence Stellar Systems, Protostars and Planets IV, ed. V. Mannings, A. P. Boss, & S. S. Russell (University of Arizona Press, Tucson), in press

Heap, S. R., Lindler, D. J., Lanz, T. M., et al. 2000, ApJ, 539, 435
Kalas, P., & Jewitt, D. 1995, AJ, 110, 794
Kalas, P., Larwood, J., Smith, B. A., & Schultz, A. 2000, ApJ, 530, L133
Karmann, C., Beust, H., & Klinger, J., A&A, 372, 616
Lagrange, A.-M., Plazy, F., Beust, H., et al. 1996, A&A, 310, 547
Lagrange, A.-M., Backman, D. E., & Artymowicz, P. 2000, Planetary Material around Main Sequence Stars, in Protostars and Planets IV, ed. V. Mannings, A. P. Boss, & S. S. Russell (University of Arizona Press, Tucson), 639
Lanz, T., Heap, S. R., & Hubeny, I. 1995, ApJ, 447, L41
Lazzaro, D., Sicardy, B., Roques, F., & Greenberg, R. 1994, Icarus, 108, 59
Lecavelier des Etangs, A., Deleuil, M., Vidal-Madjar, A., et al. 1995, A&A, 299, 557
Lecavelier des Etangs, A., Vidal-Madjar, A., & Ferlet, R. 1996, A&A, 307, 542
Levison, H. F., & Duncan, M. J. 1994, Icarus, 108, 18
Levison, H. F., Duncan, M. J., & Wetherill, G. W. 1994, Nature, 372, 441
Liou, J.-C., & Malhotra, R. 1997, Science, 275, 375
Marzari, F., & Scholl, H. 2000, ApJ, 543, 328
Moons, M. 1994, Celest. Mech. Dynam. Astron., 60, 173
Moons, M., & Morbidelli, A. 1995, Icarus, 114, 33
Morbidelli, A., & Moons, M. 1993, Icarus, 102, 316
Mouillet, D., Larwood, J. D., Papaloizou, J. C. B., & Lagrange, A.-M. 1997, MNRAS, 292, 896
Murray, N., Hansen, B., Holman, M., & Tremaine, S. 1998, Science, 279, 69
Pantin, E., Lagage, P. O., & Artymowicz, P. 1997, A&A, 327, 1123
Paresce, F. 1991, A&A, 247, L25
Petit, J.-M., & Farinella, P. 1993, Celest. Mech. Dynam. Astron., 57, 1
Pollack, J. B., Hubickyj, O., Bodenheimer, P., et al. 1996, Icarus, 124, 62
Quillen, A. C., & Holman, M. 2000, ApJ, 119, 397
Roques, F., Scholl, H., Sicardy, B., & Smith, B. A. 1994, Icarus, 108, 37
Smith, B., & Terrile, R. 1984, Science, 226, 1421
Thebault, P., & Brahic, A. 1999, Planet. Space Sci., 47, 233
Trilling, D. E., Benz, W., Guillot, T., et al. 1998, ApJ, 500, 428
Vidal-Madjar, A., Lagrange-Henri, A.-M., Feldman, P. D., et al. 1994, A&A, 290, 245
Vokrouhlický, D., & Farinella, P. 1999, AJ, 118, 3049
Vidal-Madjar, A., Lecavelier des Etangs, A., & Ferlet, R. 1998, Planet. Space Sci., 46, 629
Vogt, S. S., Marcy, G. W., Butler, R. P., & Apps, K. 2000, ApJ, 536, 902
Ward, W. R. 1997, ApJ, 482, L211
Weidenschilling, S. J. 1977, Astr. Sp. Sci., 51, 153
Wisdom, J., & Holman, M. 1991, AJ, 102, 1528
Yoshikawa, M. 1989, A&A, 213, 436